

1. REPORT NUMBER  CA21-3114-1	2. GOVERNMENT ASSOCIATION NUMBER  (Empty)	3. RECIPIENT'S CATALOG NUMBER  (Empty)
4. TITLE AND SUBTITLE Effect of Member End Eccentricity in Steel Truss Bridge Evaluation		5. REPORT DATE April, 2021
7. AUTHOR(S)  Hooseok Lee, Mathew Reynolds, Chia-Ming Uang		6. PERFORMING ORGANIZATION CODE  (Empty)
9. PERFORMING ORGANIZATION NAME AND ADDRESS Department of Structural Engineering University of California, San Diego La Jolla, California 92093		8. PERFORMING ORGANIZATION REPORT NO.  SSRP-21/03
12. SPONSORING AGENCY AND ADDRESS California Department of Transportation Division of Engineering Services 1801 30th St., MS-9-2/5i Sacramento, California 95816		10. WORK UNIT NUMBER  (Empty)
(Empty)		11. CONTRACT OR GRANT NUMBER  65A0687
(Empty)		13. TYPE OF REPORT AND PERIOD COVERED Final Report May 2018 - April 2021
(Empty)		14. SPONSORING AGENCY CODE  (Empty)

15. SUPPLEMENTARY NOTES  
 Prepared in cooperation with the State of California Department of Transportation.

16. ABSTRACT  
 Many existing steel truss bridges use built-up members that are connected by either steel pins or riveted gusset connections. Working lines, when provided in the as-built design drawings, do not necessarily coincide with the centroidal lines, creating an eccentricity,  $e$ , in the truss members. It is a common analysis practice that pin-connected truss model be created based on the working lines; such analysis would provide only axial forces in each member. To account for the eccentricity effect in truss members, which produces moments, there is no consensus-based approach. One practice used by Caltrans is to consider 100% eccentricity for pin-connected members and 50% eccentricity for gusset-connected members to calculate the member moments. Two existing bridges in California were selected in this study. Two software (Abaqus and SAP2000) were used for the finite element analysis. For the first bridge with pinned connections, field testing was used to confirm a high-fidelity Abaqus finite element model. A SAP2000 model that used beam elements and rigid links to model the eccentricity was shown to provide accurate member moments. For the second bridge with riveted gusset plat connection, a SAP2000 model that also used beam elements and rigid links to model the eccentricity produced member moments consistent to those predicted by an Abaqus model. In both bridges, it was shown that the Caltrans practice in general could not capture the double-curvature bending observed in top chord members. The moment magnitude also could not be reliably predicted by the current practice. For trusses with members connected by either steel pins or gusset connections, procedures to model a truss with beam elements and rigid links to directly include the effect of eccentricity were developed.

17. KEY WORDS Bridge, Truss, Eccentricity, Load Rating,	18. DISTRIBUTION STATEMENT No Restrictions
19. SECURITY CLASSIFICATION (of this report)  unclassified	20. NUMBER OF PAGES  89
21. COST OF REPORT CHARGED  (Empty)	

## **DISCLAIMER STATEMENT**

This document is disseminated in the interest of information exchange. The contents of this report reflect the views of the authors who are responsible for the facts and accuracy of the data presented herein. The contents do not necessarily reflect the official views or policies of the State of California or the Federal Highway Administration. This publication does not constitute a standard, specification or regulation. This report does not constitute an endorsement by the Department of any product described herein.

For individuals with sensory disabilities, this document is available in alternate formats. For information, call (916) 654-8899, TTY 711, or write to California Department of Transportation, Division of Research, Innovation and System Information, MS-83, P.O. Box 942873, Sacramento, CA 94273-0001.



**STRUCTURAL SYSTEMS  
RESEARCH PROJECT**

Report No.  
SSRP-21/03

**Effect of Member End Eccentricity in Steel Truss  
Bridge Evaluation**

by

**Hooseok Lee  
Mathew Reynolds  
Chia-Ming Uang**

Final Report Submitted to California Department of Transportation

April 2021

Department of Structural Engineering  
University of California, San Diego  
La Jolla, California 92093

University of California, San Diego  
Department of Structural Engineering  
Structural Systems Research Project

Report No. SSRP-21/03

**Effect of Member End Eccentricity in Steel Truss Bridge  
Evaluation**

by

**Hooseok Lee**

*Graduate Student Researcher*

**Mathew Reynolds**

*Former Graduate Student Researcher*

**Chia-Ming Uang**

*Professor of Structural Engineering*

Final Report Submitted to California Department of Transportation

Department of Structural Engineering  
University of California, San Diego  
La Jolla, California 92093

## **DISCLAIMER**

This document is disseminated in the interest of information exchange. The contents of this report reflect the views of the authors who are responsible for the facts and accuracy of the data presented herein. The contents do not necessarily reflect the official views or policies of the State of California or the Federal Highway Administration. This publication does not constitute a standard, specification or regulation. This report does not constitute an endorsement by the Department of any product described herein.

For individuals with sensory disabilities, this document is available in alternate formats. For information, call (916) 654-8899, TTY 711, or write to California Department of Transportation, Division of Research, Innovation and System Information, MS-83, P.O. Box 942873, Sacramento, CA 94273-0001.

## **ACKNOWLEDGEMENTS**

The California Department of Transportation (Caltrans) funded this work under Contract #65A0687. We would like to thank Dr. George Huang (project manager) for his guidance and advice. The authors would like to acknowledge Caltrans for assisting in field testing of the Bridge Road over Santa Paula Creek. Mr. Michael Sanders from the Charles Lee Powell Structures Laboratories at the University of California, San Diego, supported instrumentation and field testing of the bridge.

## ABSTRACT

Many existing steel truss bridges use built-up members that are connected by either steel pins or riveted gusset connections. Working lines, when provided in the as-built design drawings, do not necessarily coincide with the centroidal lines, creating an eccentricity,  $e$ , in the truss members. In a structural analysis, it is a common practice that a pin-connected truss model be created based on the working lines; such analysis would provide only axial forces in each member. To account for the eccentricity effect in truss members, which produces moments, there is no consensus-based approach. One practice used by Caltrans is to consider 100% eccentricity for pin-connected members and 50% eccentricity for gusset-connected members to calculate the member moments.

Two existing bridges in California were selected in this study. The pin-connected Bridge Road over Santa Paula Creek was evaluated by both finite element analysis and field testing. Finite element analysis was conducted on the Bridge Road over Klamath River, located in Siskiyou County, which uses riveted gusset plates to connect members. Two software (Abaqus and SAP2000) were used for the finite element analysis.

For the first bridge, field testing was used to confirm a high-fidelity Abaqus finite element model. A SAP2000 model that used beam elements and rigid links to model the eccentricity was shown to provide accurate member moments. For the second bridge, a SAP2000 model that also used beam elements and rigid links to model the eccentricity produced member moments consistent to those predicted by an Abaqus model. In both bridges, it was shown that the Caltrans practice in general could not capture the double-curvature bending observed in most top chord members. In addition to the direction of bending, the moment magnitude also could not be reliably predicted by the current practice.

For trusses with members connected by either steel pins or gusset connections, procedures to model a truss with beam elements and rigid links to directly include the effect of eccentricity were developed. The analyses performed in this study were based on a vehicle at specific locations. To evaluate the level of conservatism or non-conservatism for bridge rating using the current practice, case study of sample truss bridges with the recommended modeling procedures is needed. The effect of using the live load response envelope for computing the rating factor should also be investigated.

# TABLE OF CONTENTS

<b>DISCLAIMER.....</b>	<b>iii</b>
<b>ACKNOWLEDGEMENTS .....</b>	<b>iv</b>
<b>ABSTRACT.....</b>	<b>v</b>
<b>TABLE OF CONTENTS .....</b>	<b>vi</b>
<b>LIST OF FIGURES .....</b>	<b>viii</b>
<b>LIST OF TABLES .....</b>	<b>xi</b>
<b>1 INTRODUCTION .....</b>	<b>1</b>
1.1 Research Background .....	1
1.2 Research Objective and Scope.....	2
<b>2 BRIDGE ROAD OVER SANTA PAULA CREEK: FINITE ELEMENT ANALYSIS .....</b>	<b>4</b>
2.1 General.....	4
2.2 Description of Bridge .....	4
2.3 Abaqus Modeling.....	4
2.4 SAP2000 Modeling .....	5
2.5 Analysis Results.....	5
2.5.1 SAP2000 Analysis .....	5
2.5.2 Abaqus Analysis .....	6
2.5.3 Caltrans Practice .....	6
2.6 Insight of Member End Moments.....	7
<b>3 BRIDGE ROAD OVER SANTA PAULA CREEK: FIELD TESTING .....</b>	<b>33</b>
3.1 General.....	33
3.2 Instrumentation .....	33
3.3 Loading Condition.....	33
3.4 Data Reduction .....	34
3.5 Results of Field Testing.....	34
3.6 Correlation Study.....	35
<b>4 BRIDGE ROAD OVER KLAMATH RIVER .....</b>	<b>50</b>
4.1 General.....	50

4.2	Description of Bridge .....	50
4.3	Abaqus Analysis .....	50
4.4	SAP2000 Analysis.....	51
4.4.1	General.....	51
4.4.2	Model 1 .....	51
4.4.3	Model 2 .....	52
4.5	Caltrans Practice .....	53
4.6	Effect of Retrofit.....	53
<b>5</b>	<b>SUMMARY AND CONCLUSIONS .....</b>	<b>73</b>
5.1	Summary.....	73
5.2	Conclusions.....	74
5.2.1	Pin-connected Bridge Road over Santa Paula Creek .....	74
5.2.2	Gusset-connected Bridge Road over Klamath River .....	74
5.3	Recommended Truss Modeling Procedures .....	75
5.4	Future Study.....	76
	<b>REFERENCES.....</b>	<b>77</b>

## LIST OF FIGURES

Figure 1.1 Example a Built-up Member with an Asymmetry for Bending in Plane .....	3
Figure 2.1 The Bridge Road over Santa Paula Creek .....	11
Figure 2.2 Elevation of Truss and Joint Designation.....	12
Figure 2.3 Cross Section of Bridge.....	12
Figure 2.4 Pin-connected Eyebars (Bottom Chord and Diagonal Brace).....	13
Figure 2.5 Pin Joints at U1, U2, and L0.....	13
Figure 2.6 Cross Sections of Built-up Members.....	15
Figure 2.7 Elevation View of Abaqus Model .....	15
Figure 2.8 Modeling of Built-up Member .....	16
Figure 2.9 Modelling Detail at Joint U1 (Top Cover Plates Removed for Clarity).....	16
Figure 2.10 Detail at Joint U1 .....	17
Figure 2.11 Detail at Joint U2.....	18
Figure 2.12 Detail at Joint L0 .....	19
Figure 2.13 Detail at Joint L3 .....	20
Figure 2.14 Load Cases.....	21
Figure 2.15 SAP2000 Truss Model .....	22
Figure 2.16 Comparison of Vertical Deflection Profiles .....	23
Figure 2.17 SAP2000 Analysis Results: Member Axial Forces.....	24
Figure 2.18 SAP2000 Analysis Results: Member Shear Forces .....	25
Figure 2.19 SAP2000 Analysis Results: Internal Forces of Members L0U1 and U1U2 (Load Case 1).....	26
Figure 2.20 SAP2000 Analysis Results: Internal Forces of Members L0U1 and U1U2 (Load Case 2).....	27
Figure 2.21 Distribution of Moment and Axial Force (Load Case 1) .....	28
Figure 2.22 Distribution of Moment and Axial Force (Load Case 2) .....	29
Figure 2.23 Comparison of Moments Based on SAP2000 and Caltrans Practice .....	30
Figure 2.24 Determination of End Post Moment by Statics (Load Case 1) .....	31
Figure 2.25 Determination of Member U1U2 Moment by Statics (Load Case 1) .....	32
Figure 3.1 Instrumentation Elevation .....	37

Figure 3.2 Instrumentation Section.....	37
Figure 3.3 Surface Preparation .....	38
Figure 3.4 Data Acquisition System.....	38
Figure 3.5 Water Truck for Load Tests .....	39
Figure 3.6 Truck Loading for Field Tests.....	40
Figure 3.7 Recorded Strain Gage Data (Load Case 1).....	41
Figure 3.8 Recorded Strain Gage Data (Load Case 2).....	42
Figure 3.9 Distribution of Moment and Axial Force from Field Testing (Load Case 1) .	43
Figure 3.10 Distribution of Moment and Axial Force from Field Testing (Load Case 2)	44
Figure 3.11 Vertical Deflection of Truss from Field Testing.....	45
Figure 3.12 Comparison of Vertical Deflections.....	46
Figure 3.13 Comparison of Moments and Axial Forces (Load Case 1).....	47
Figure 3.14 Comparison of Moments and Axial Forces (Load Case 2).....	48
Figure 3.15 Effect of Friction in Pin Joint U1 (Load Case 1).....	49
Figure 4.1 The Bridge Road over Klamath River.....	57
Figure 4.2 Elevation of Truss and Member Designation.....	58
Figure 4.3 Cross Section of Bridge.....	58
Figure 4.4 As-built Drawing.....	59
Figure 4.5 Gusset Joints at U2 .....	60
Figure 4.6 Cross Sections of Built-up Members.....	60
Figure 4.7 Detail at Joint U1.....	61
Figure 4.8 Detail at Joint U2.....	62
Figure 4.9 Loading Cases .....	63
Figure 4.10 Comparison of Vertical Deflection Profiles .....	64
Figure 4.11 Distribution of Moment and Axial Force (Load Case 1) .....	65
Figure 4.12 Distribution of Moment and Axial Force (Load Case 2) .....	66
Figure 4.13 SAP2000 Model of the Truss (Model 1).....	67
Figure 4.14 SAP2000 Model of the Truss (Model 2).....	67
Figure 4.15 Free-body Diagram at Joint U1 .....	68
Figure 4.16 Free-body Diagram at Joint U3 .....	69
Figure 4.17 Free-body Diagram at Joint L0.....	70

Figure 4.18 Comparison of Moments Based on SAP2000 and Caltrans Practice ..... 71  
Figure 4.19 Comparison of Retrofitted and Non-Retrofitted..... 72

## LIST OF TABLES

Table 2.1 Truss Member Sizes.....	9
Table 2.2 Moments and Axial Forces from Abaqus .....	9
Table 2.3 Moments and Axial Forces from SAP2000 Analysis.....	10
Table 2.4 Vertical Deflections of Truss .....	10
Table 3.1 Moment and Axial Force from Field Testing .....	36
Table 3.2 Vertical Deflection of Bridge from Field Tests .....	36
Table 4.1 Truss Member Sizes.....	54
Table 4.2 Moments and Axial Forces from Abaqus .....	54
Table 4.3 Moments and Axial Forces from SAP2000 (Model 1).....	55
Table 4.4 Moments and Axial Forces from SAP2000 (Model 2).....	55
Table 4.5 Vertical Deflection of Bridge .....	56

# 1 INTRODUCTION

## 1.1 Research Background

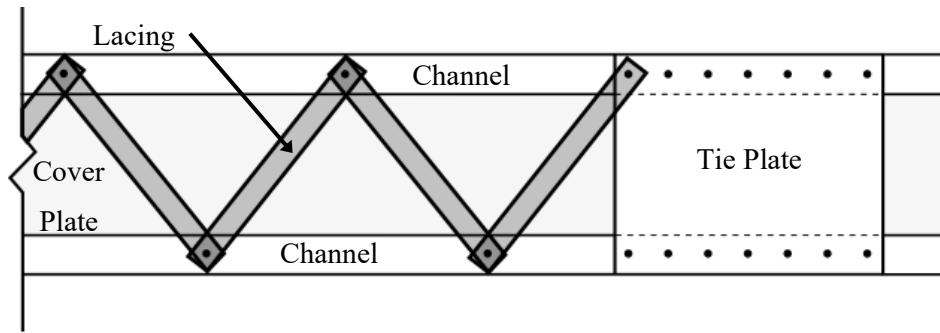
Steel truss bridges were the preferred type of bridge for many crossings throughout the twentieth century until changes in the availability of high-performance steels and an increased cost of labor pushed designers towards other bridge types. Therefore, even though the construction of new steel truss bridges is rare, there are many existing structures in California that undergo routine inspection and evaluation. Many of these older structures are fabricated using built-up members due to the lack of availability of large rolled sections and the relatively inexpensive labor cost to assemble the members at that time.

The built-up members typically consist of smaller rolled shapes such as channels and angles spaced apart by continuous or discrete plates. Discrete plates were either single orthogonal pieces spaced down the length of the member (battens) or were diagonally orientated flat bars (lacing). Refer to Figure 1.1 for a built-up section, where the mid-depth of the channels is used to define the working line. Often the cross sections of built-up members forming the top chord of the truss are not symmetric about the axis of in-plane bending. This is due to the tendency of designers to use solid top cover plates and battens or lacing to brace the bottom of the member (Figure 1.1). The asymmetry of the member leads to there being a difference (i.e., eccentricity,  $e$ ) between centroid of the cross section and the working line. To account for the additional flexural demands, designers treat the eccentricity with different approaches. For example, the full eccentricity is used by Caltrans when the end connection of member is a steel pin, and half the eccentricity is used when the end connection of the member is made through gusset plates with conventional fasteners like rivets or bolts. Some other bridge owners neglect the eccentricity altogether and evaluate the member as an axially loaded member.

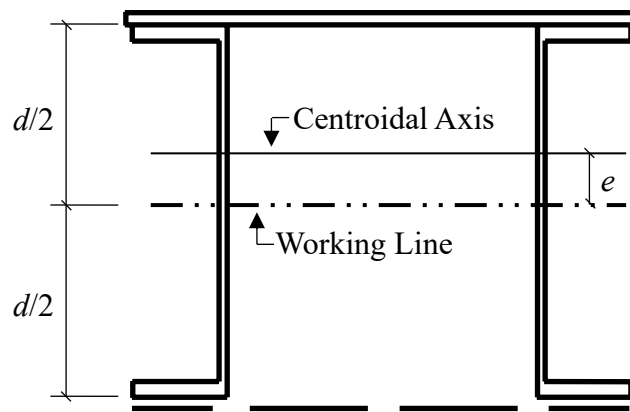
Although the eccentricity is small, the additional end moments imposed can have a large effect due to the relatively low flexural capacity of built-up riveted members and the large axial forces driving the first-order and second-order flexural demands. This may lead to the conclusion that the bridge should be retrofitted or posted.

## **1.2 Research Objective and Scope**

The objective of this research is to verify design assumptions commonly used by bridge engineers. Two steel truss bridges are investigated. The Bridge Road over Santa Paula Creek, located in Ventura County, has been identified as a typical steel truss bridge that consist of pin connections. The second one is the Bridge Road over Klamath River located in Siskiyou County; this bridge features steel trusses with riveted gusset connections. Finite element analyses using both the high-fidelity software Abaqus CAE (Abaqus, 2014) and a commonly used engineering software SAP2000 (CSI, 2019) are used to evaluate the member force demands for both bridges. To verify the accuracy of the Abaqus predictions, field testing of the first bridges is also conducted. Analysis results are then used to validate the adequacy of the Caltrans practice for member end moment calculations.



(a) Underside



(b) Cross Section

Figure 1.1 Example a Built-up Member with an Asymmetry for Bending in Plane

## 2 BRIDGE ROAD OVER SANTA PAULA CREEK: FINITE ELEMENT ANALYSIS

### 2.1 General

The 132-ft long Bridge Road over Santa Paula Creek (Structure No. 52C0053), located in Ventura County, California is a typical through Pratt truss bridge that was constructed in 1941. The bridge features built-up members interconnected by pins. Both finite element analysis and field testing were conducted on this bridge. This chapter presents the results of finite element analysis. Field testing is to be presented in the next chapter.

### 2.2 Description of Bridge

Figure 2.1 shows the bridge in its existing condition; the structural conditions were listed as Good in Caltrans 2010 Bridge Inspection Report. This single-span truss bridge sits on gravity wall abutments. Figure 2.2 depicts the elevation of the truss. The cross section of the bridge is shown in Figure 2.3. The bridge features timber deck plank and stringers (4×20, 21 total) and I20×70 steel floor beams. A7 steel was probably specified for the trusses because  $F_y = 30$  ksi was used in the Caltrans 2010 rating analysis.

The cross section of each member is summarized in Table 2.1. Pin-connected tension bars are used for the bottom chords and diagonal braces (Figure 2.4). Pins are used at each joint (Figure 2.5). Cross sectional dimensions of four types of built-up members used in this bridge are summarized in Figure 2.6. Note that pins are located at the mid-height of the double-channel sections for the end posts and top chord. With a cover plate at the top face only and lacing at the bottom face, the centroid is 1.692 in. above the mid-height, i.e., the eccentricity,  $e$ , for these members is 1.692 in. Following the common practice, lacing was ignored in calculating the cross-sectional properties.

### 2.3 Abaqus Modeling

The software package Abaqus CAE (Abaqus, 2014) was used for a more detailed finite element analysis. This software is capable of simulating the response of a 3-D structure that responds in both the elastic and inelastic ranges that considers the large-

deformation effect including buckling. For this study, elastic response is expected and only one truss of the bridge is modeled.

Figure 2.7 shows an overall view of the Abaqus model. Four-node quadrilateral shell element (S4R) with reduced integration was used to model all members and connecting plates. An example finite element mesh of the top chord (or end post) with two channels, one top cover plate, and lacing at the bottom face is shown in Figure 2.8. Each rivet was also modeled by using the point-based “Fastener” in Abaqus. At a pin joint, a reference point of connecting member was first defined; these reference points were then connected by using the “Hinge” feature in Abaqus to allow for relative rotation among members (Figure 2.9). With this feature, pins need not be modeled physically. Abaqus models at selected joints are presented in Figure 2.10 to Figure 2.13. Note that diagonal members other than end posts are tension-only members. Eyebars are used for the bottom chord.

To evaluate member forces, two load conditions used in the field testing (see Chapter 3) were applied to the Abaqus model (Figure 2.14).

## **2.4 SAP2000 Modeling**

While very powerful, Abaqus is more suitable for research. Instead, software like SAP2000 (CSI, 2019) that uses beam or truss element for truss analysis is more practical for routine design and evaluation. In this research, SAP2000 models were also created. Beam element was used for all the members. In defining the geometry of the truss, the working line was assumed to pass through the pins. Two models were created, one without and one with member eccentricity as shown in Figure 2.15. For the latter case, rigid links were included to account for the eccentricity between the pin and centroidal axis of the cross section. The load conditions were the same as those used in the Abaqus analysis.

## **2.5 Analysis Results**

### **2.5.1 SAP2000 Analysis**

A comparison of the vertical deflection profiles along the span of the truss in Figure 2.16 shows that the predicted global responses from both Abaqus and SAP2000 are very similar. Figure 2.17 compares the member axial forces for cases with and without eccentricity considered. As expected, axial forces are very similar. Figure 2.18 shows the shear force distribution. Since higher shear forces exist in the rigid links connected to joints

U1 and L0, large member end moments there would occur; the end moment equals the link shear times the eccentricity,  $e$ . See the moment diagrams of top chord U1U2 and end post L0U1 for both loading cases in Figure 2.19 and Figure 2.20, respectively. It is observed that the end post is in a uniform bending and the top chord U1U2 is bent in reverse curvature.

### 2.5.2 Abaqus Analysis

Resultant forces at a section along the member can be computed by integrating stresses along the depth of the section. The computed axial force and bending moment diagrams for the top chords are presented in Figure 2.21 and Figure 2.22 for Load Cases 1 and 2, respectively; also see Table 2.2 and Table 2.3 for the tabulated values. The bending moment distribution is comparable to that predicted by SAP2000 when the eccentricity is included in the model. The predicted internal forces, especially the bending moments, are to be verified by field testing (see Chapter 3).

### 2.5.3 Caltrans Practice

For a bridge truss with pin joints, the practice of Caltrans is to ignore the end eccentricity in a truss analysis, and then multiply the member axial forces by 100% of the end eccentricity to compute member end moments. Based on this procedure, which always produces uniform bending, moment diagrams for both loading cases are compared with those predicted by SAP2000.

Figure 2.23 shows that the Caltrans practice does not capture the magnitude and distribution of the moment diagrams. For end post L0U1, the Caltrans practice can predict the uniform bending and the moment magnitude (the reason is to be explained in the next section.) But this is not the case for the top chord members. For U1U2 and U2U3, the Caltrans practice cannot predict the double curvature and the moment magnitudes. Field testing to be presented in Chapter 3 aims to verify the moment diagrams and the associated curvatures predicted by the finite element analyses.

Moment gradient will affect the P- $\delta$  effect of the member. According to Section 4.5.3.2.2b of the AASHTO LRFD Specification (AASHTO 2017), the moment magnifier for braced mode deflection is

$$\delta_b = \frac{C_m}{1 - \frac{P_u}{\phi_K P_e}} \geq 1.0 \quad (2.1)$$

where the moment gradient coefficient,  $C_m$ , equals

$$C_m = 0.6 + 0.4 \left( \frac{M_{1b}}{M_{2b}} \right) \quad (2.2)$$

$M_{1b}/M_{2b}$  is taken as positive for single curvature and negative for double curvature. Consider top chord U1U2 with Load Case 1 for example. The value of  $C_m$  equals 1.0 based on the Caltrans practice because the moment diagram is uniform. Therefore, the value of  $\delta_b$ , which is a function of the axial compression force, will be always larger than 1.0. With the moment gradient shown in Figure 2.23(a), however,

$$C_m = 0.6 - 0.4 \left( \frac{40.6}{64.0} \right) = 0.346 \quad (2.3)$$

By inspection,  $\delta_b$  can be taken as 1.0 (i.e., no moment magnification) because the calculated value is less than 1.0. Therefore, the Caltrans practice tends to overestimate the P- $\delta$  effect at the member level.

## 2.6 Insight of Member End Moments

In bridge evaluation, it is not a common Caltrans practice to model member end eccentricity like that in Figure 2.15(b) in a truss analysis due to the limitations of the software used. An insight into the source of member end moment is provided below.

### End Post L0U1

It was shown in the previous section that the Caltrans practice can reliably predict the moment magnitude and the direction of curvature of L0U1. This can be explained by the statics as follows. First cut Section A-A through the upper rigid link as shown in Figure 2.24(a) to obtain a free-body shown in Figure 2.24(b). Assuming the reaction and the axial force of the bottom chord L0L1 are the same as those from a truss analysis without eccentricity. Use statics to determine the link shear,  $V_1$ , which equals 32.78 kips. Multiply this link shear by the eccentricity ( $e = 1.692$  in.) gives a moment of 55.5 kip-in. at the upper end of the end post. This moment matches that from the truss analysis with eccentricity modeled.

### Top Chord U1U2

Figure 2.25 shows the free-body used to calculate the shear ( $V_2 = 38.17$  kips) in the rigid link at joint U1. The calculated moment at the top end is 64.58 kip-in. ( $= 38.17 \times e$ ), which is very close to that (64.02 kip-in.) calculated from SAP2000. But there is no easy way to determine the moment at the U2 end of the member by statics, one reason being that it is difficult to calculate the shear in the rigid link at U2 by statics.

Table 2.1 Truss Member Sizes

Member Designation	Cross Section
L0U1, L7U6 (end posts) U1 to U6 (top chords)	2C10×15.3 + PL5/16×14
L0 to L2, L5 to L7 (bottom chords)	Bars 3½×¾ (2 total)
L2L3, L4L5 (bottom chords)	Bars 4×1-1/8 (2 total)
L3L4 (bottom chords)	Bars 4×1-1/4 (2 total)
U1L2, U6L5 (diagonals)	Bars 3-1/4×¾ (2 total)
U2L3, U5L4 (diagonals)	Bars 2-1/2×5/8 (2 total)
U3L4, U4L3 (diagonals)	Bars 7/8×7/8 (2 total)
U1L1, U6L6 (verticals)	2C6×8.2
U2L2, U3L3, U4L4, U5L5 (verticals)	2C6×8.2

Table 2.2 Moments and Axial Forces from Abaqus

Member	Location from Left Joint (in.)	Load Case 1		Load Case 2	
		$M_x$ (kip-in.)	$P$ (kips)	$M_x$ (kip-in.)	$P$ (kips)
L0U1	50	57.6	-32.8	45.7	-26.2
	150	59.4		46.8	
	250	58.3		46.1	
U1U2	254	50.2	-37.8	47.5	-35.2
	329	16.6		18.1	
	412	-20.8		-14.8	
U2U3	484	-34.4	-35.3	-11.6	-46.7
	556	-24.7		-17.5	
	623	-14.9		-22.4	
U3U4	703	-9.0	-33.1	-26.5	-43.8

Table 2.3 Moments and Axial Forces from SAP2000 Analysis

Member	Location from Left Joint (in.)	Load Case 1		Load Case 2	
		$M_x$ (kip-in.)	$P$ (kips)	$M_x$ (kip-in.)	$P$ (kips)
L0U1	0	55.5	-32.8	44.4	-26.2
	326.9	55.5	[-32.8] <sup>a</sup>	44.4	[-26.2] <sup>a</sup>
U1U2	326.9	64.0	-37.8	59.6	-35.2
	548.9	-40.6	[-38.2] <sup>a</sup>	-31.7	[-35.6] <sup>a</sup>
U2U3	548.9	-44.8	-35.4	-12.2	-46.8
	770.9	3.1	[-35.6] <sup>a</sup>	-23.3	[-47.1] <sup>a</sup>
U3U4	770.9	-4.1	-31.1 [-31.3] <sup>a</sup>	-28.8	-43.5 [-43.8] <sup>a</sup>

<sup>a</sup>for truss without eccentricity

Table 2.4 Vertical Deflections of Truss

Location (in.)	Load Case 1		Load Case 2	
	Abaqus (in.)	SAP2000 (in.)	Abaqus (in.)	SAP2000 (in.)
0	0	0	0	0
222	0.22	0.21	0.19	0.18
444	0.37	0.36	0.36	0.36
666	0.39	0.37	0.52	0.51
888	0.29	0.30	0.45	0.46
1110	0.19	0.19	0.29	0.29
1332	0.09	0.10	0.15	0.15
1554	0	0	0	0



(a) End View



(b) Side View

Figure 2.1 The Bridge Road over Santa Paula Creek

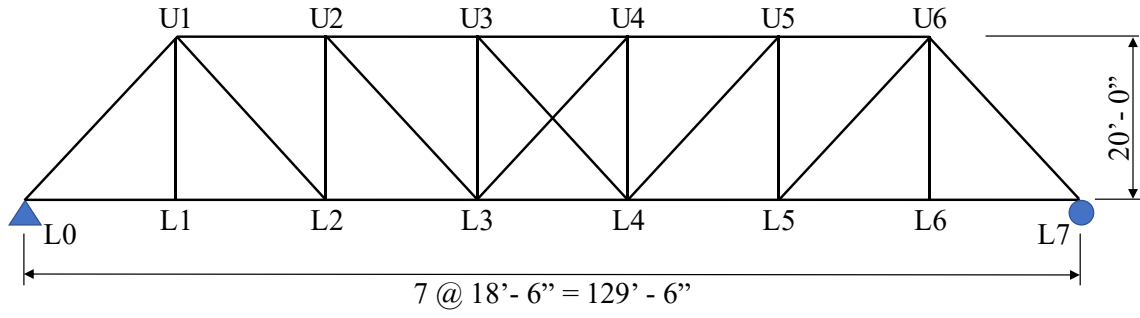


Figure 2.2 Elevation of Truss and Joint Designation

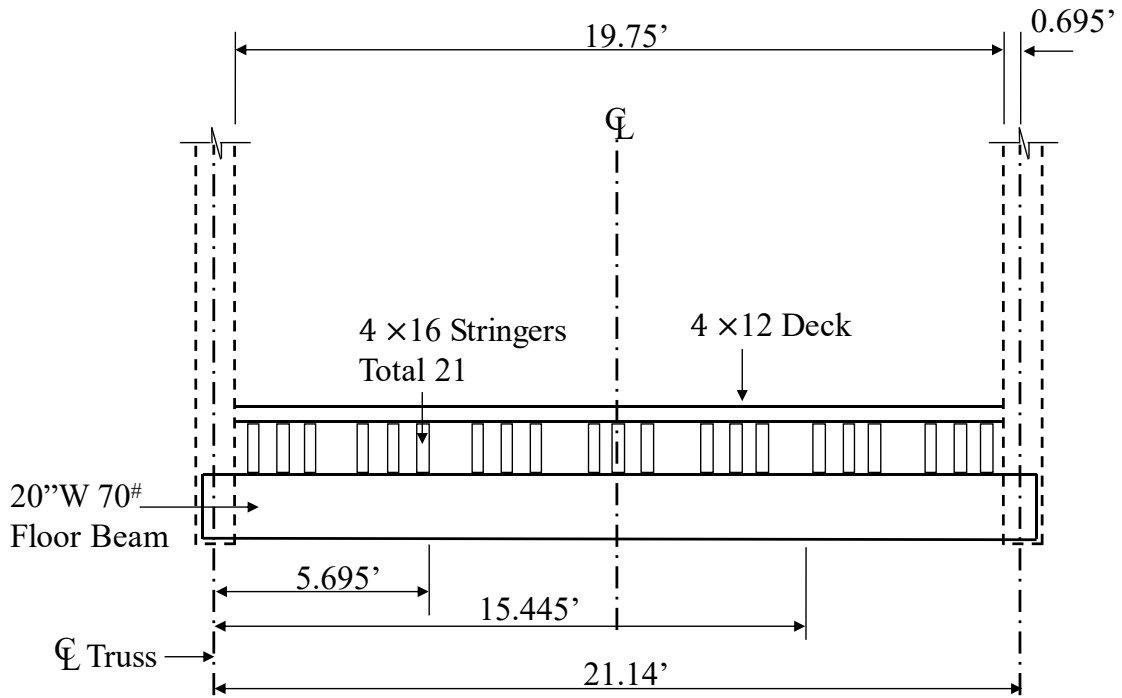


Figure 2.3 Cross Section of Bridge



Figure 2.4 Pin-connected Eyebars (Bottom Chord and Diagonal Brace)



(a) Joint U1

Figure 2.5 Pin Joints at U1, U2, and L0



(b) Joint U2



(c) Support L0

Figure 2.5 Pin Joints at U1, U2, and L0 (continued)

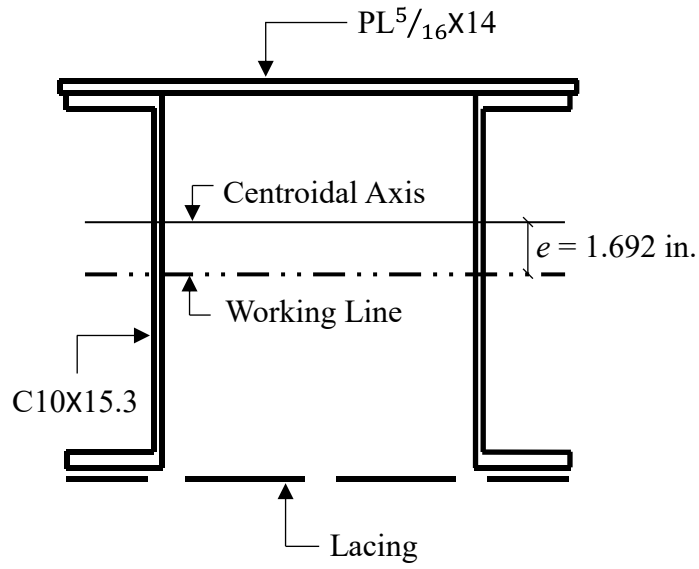


Figure 2.6 Cross Sections of Built-up Members

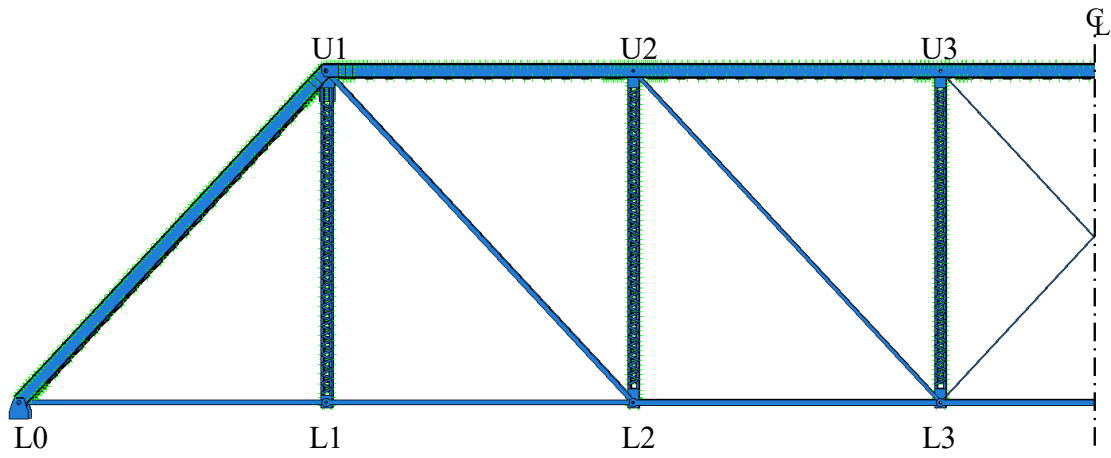


Figure 2.7 Elevation View of Abaqus Model

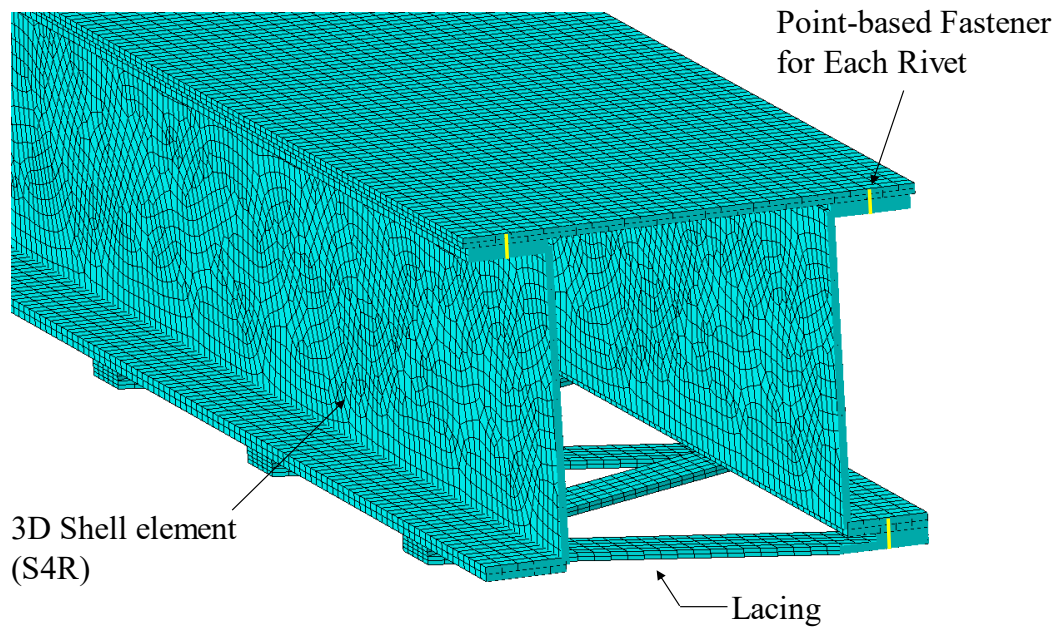


Figure 2.8 Modeling of Built-up Member

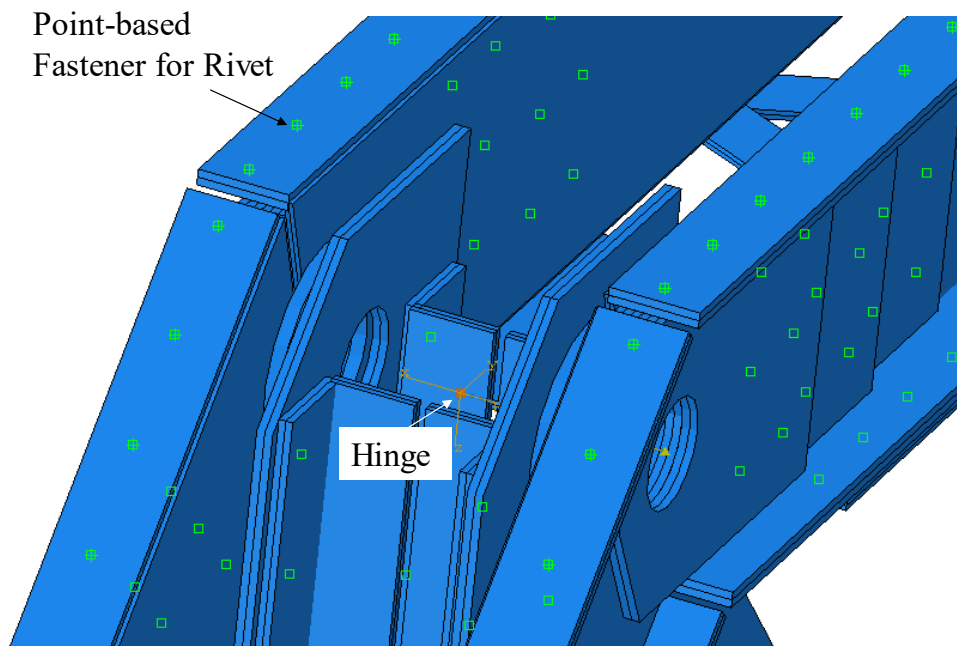
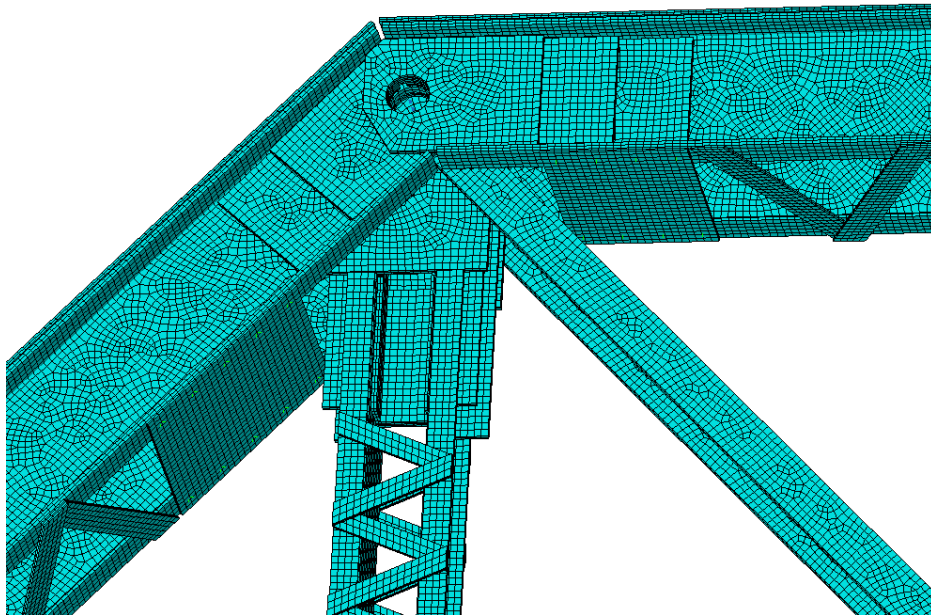


Figure 2.9 Modelling Detail at Joint U1 (Top Cover Plate Removed for Clarity)



(a) Actual

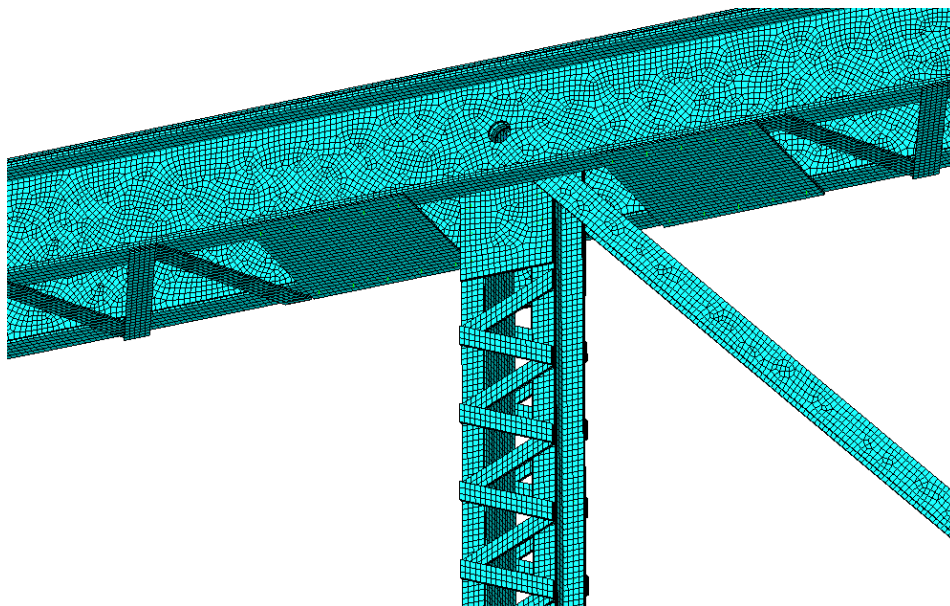


(b) Model

Figure 2.10 Detail at Joint U1



(a) Actual

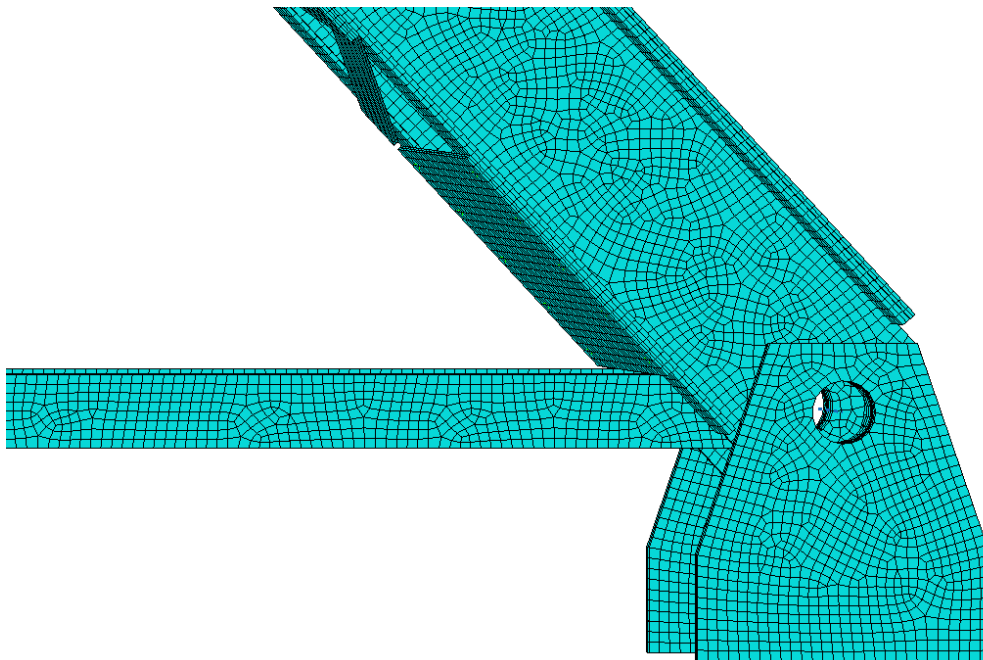


(b) Model

Figure 2.11 Detail at Joint U2



(a) Actual

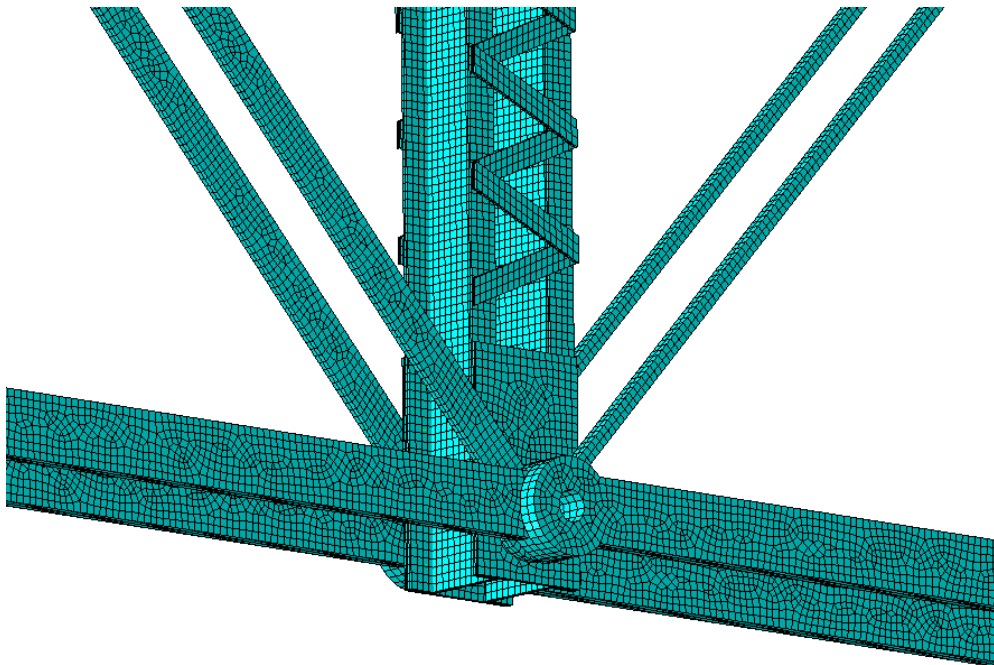


(b) Model

Figure 2.12 Detail at Joint L0

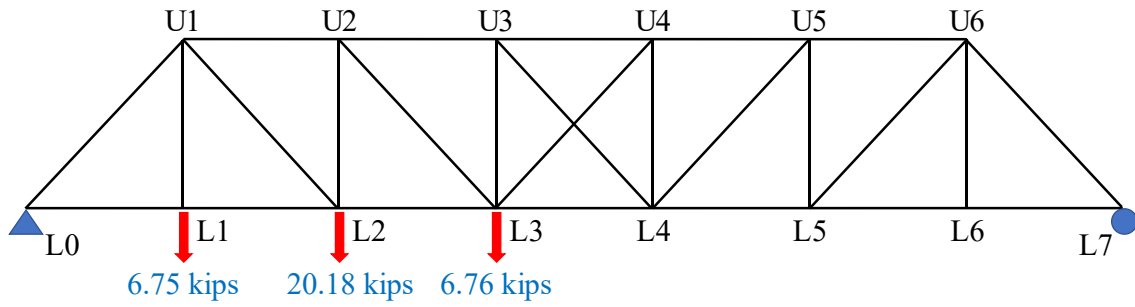


(a) Actual

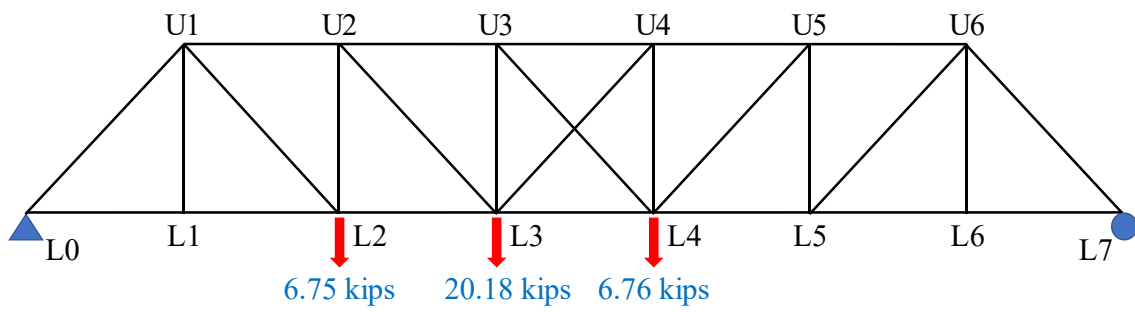


(b) Model

Figure 2.13 Detail at Joint L3

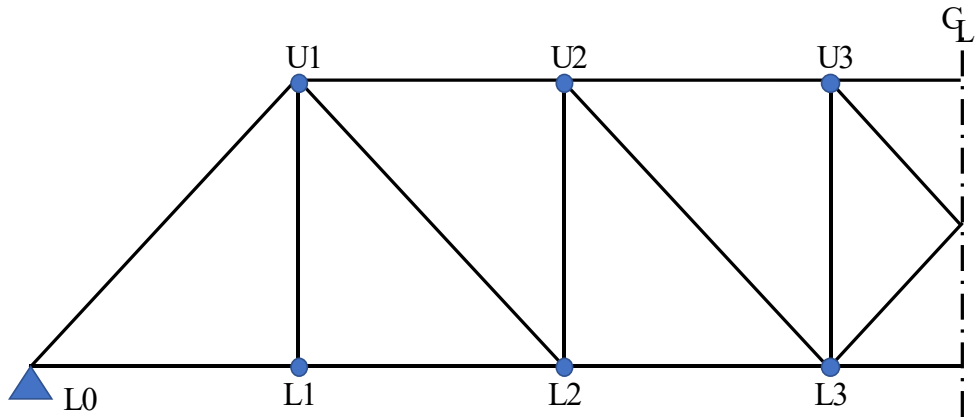


(a) Load Case 1

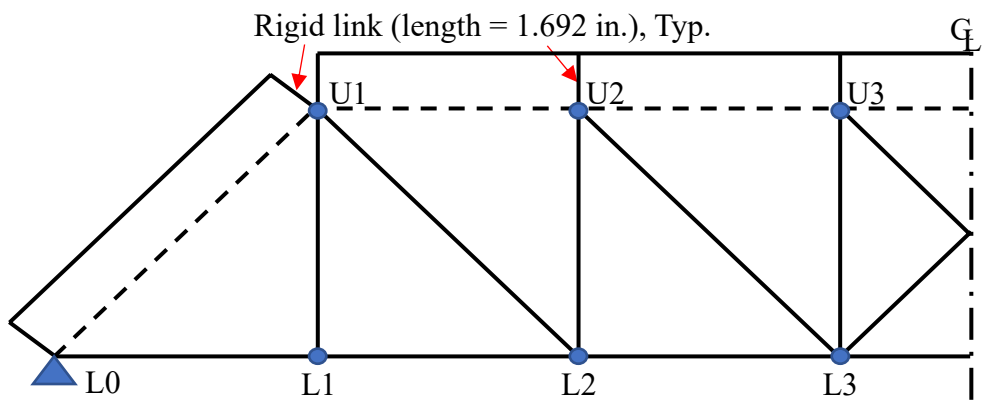


(b) Load Case 2

Figure 2.14 Load Cases

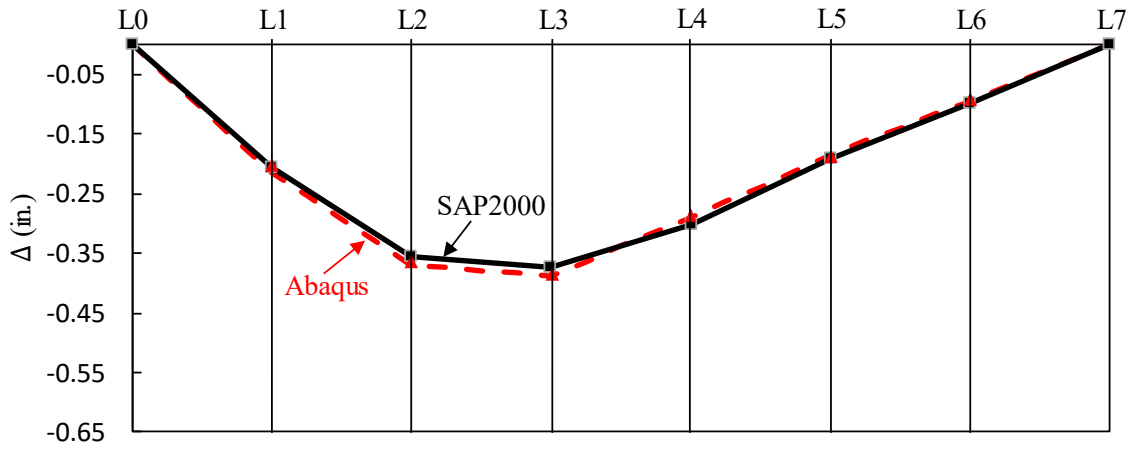


(a) without Member Eccentricity

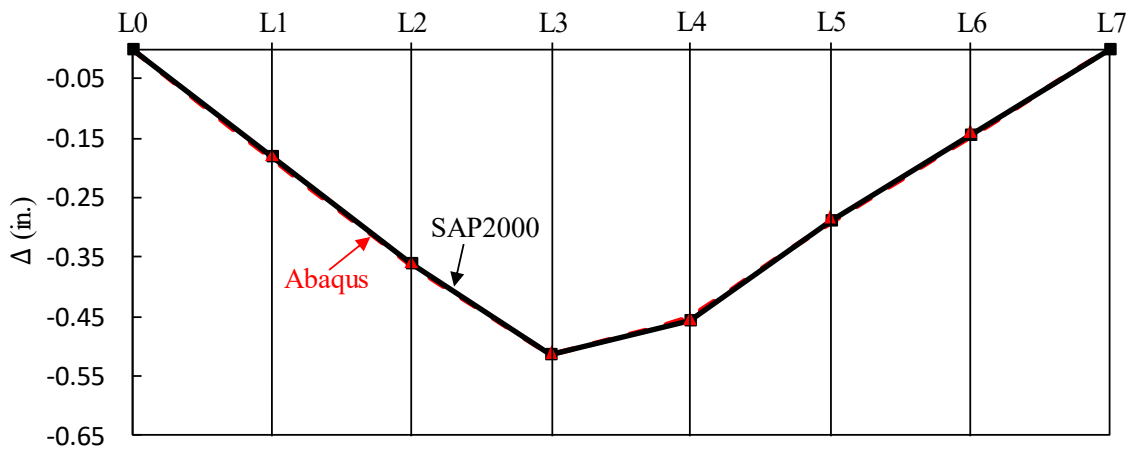


(b) with Member Eccentricity

Figure 2.15 SAP2000 Truss Model

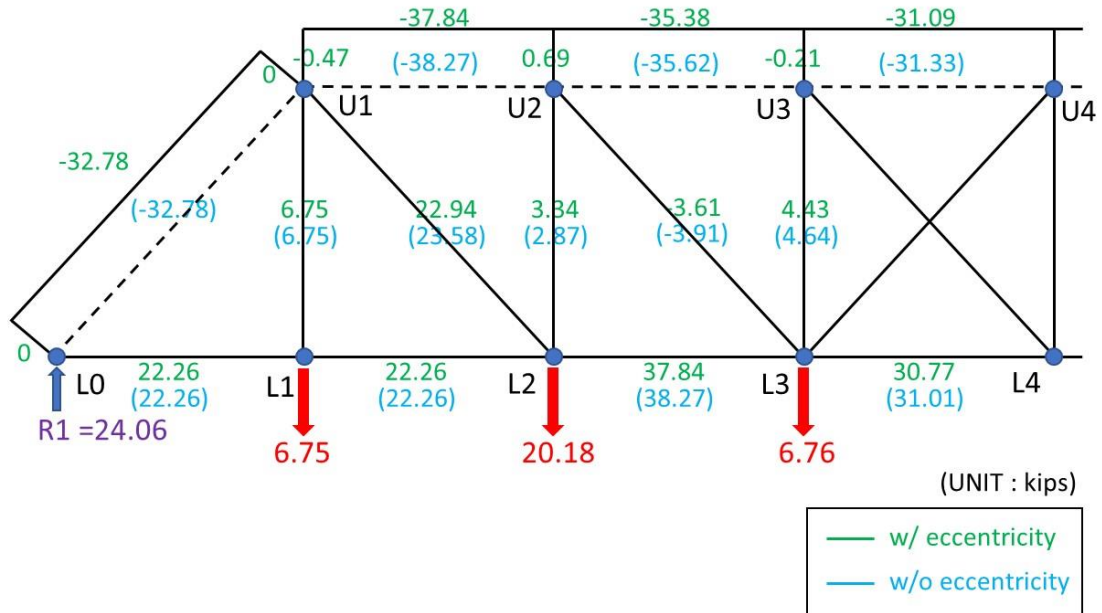


(a) Load Case 1

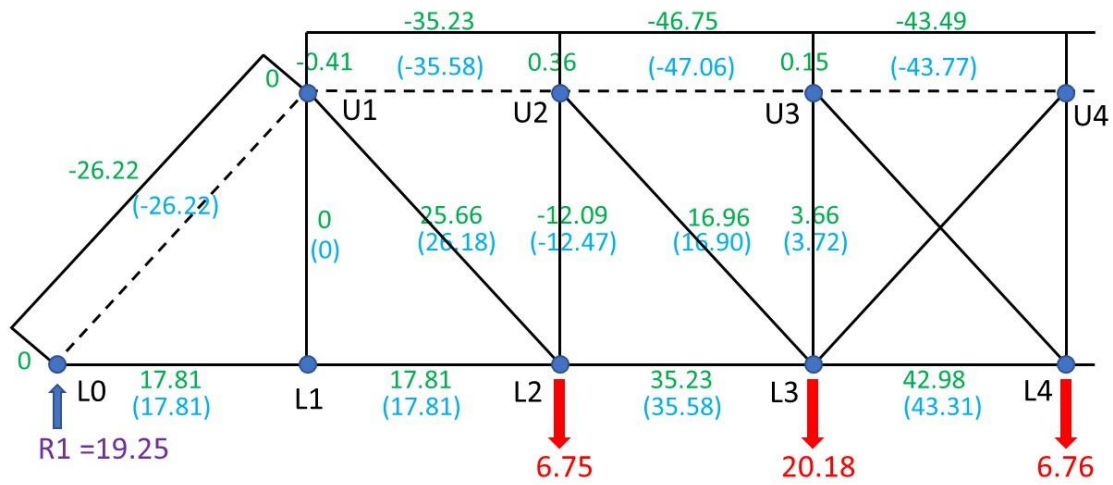


(b) Load Case 2

Figure 2.16 Comparison of Vertical Deflection Profiles



(a) Load Case 1



(b) Load Case 2

Figure 2.17 SAP2000 Analysis Results: Member Axial Forces

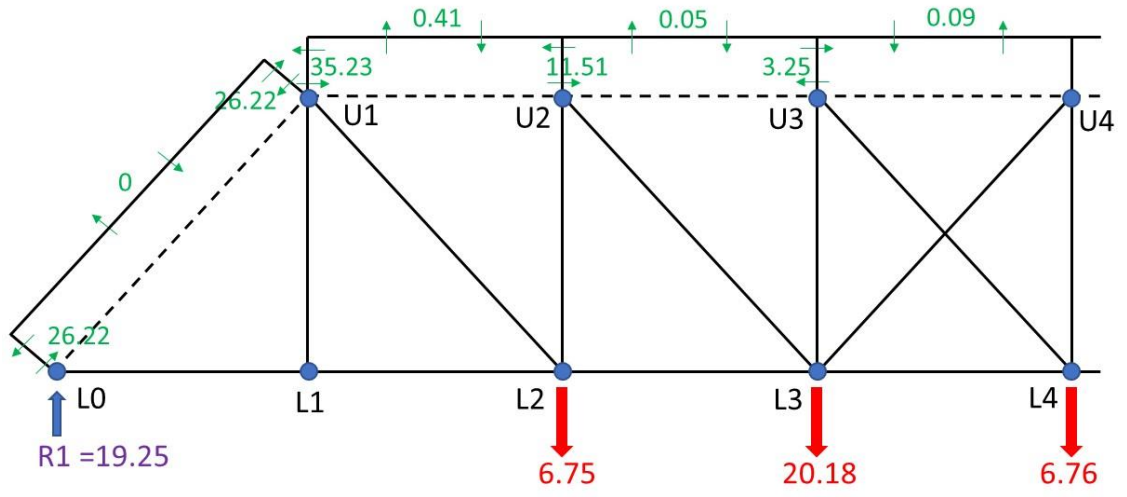
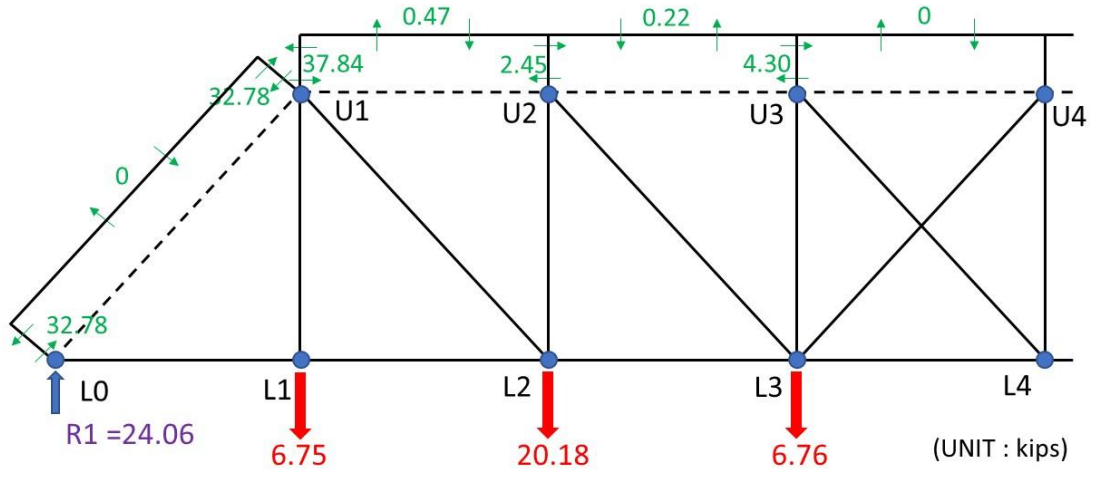
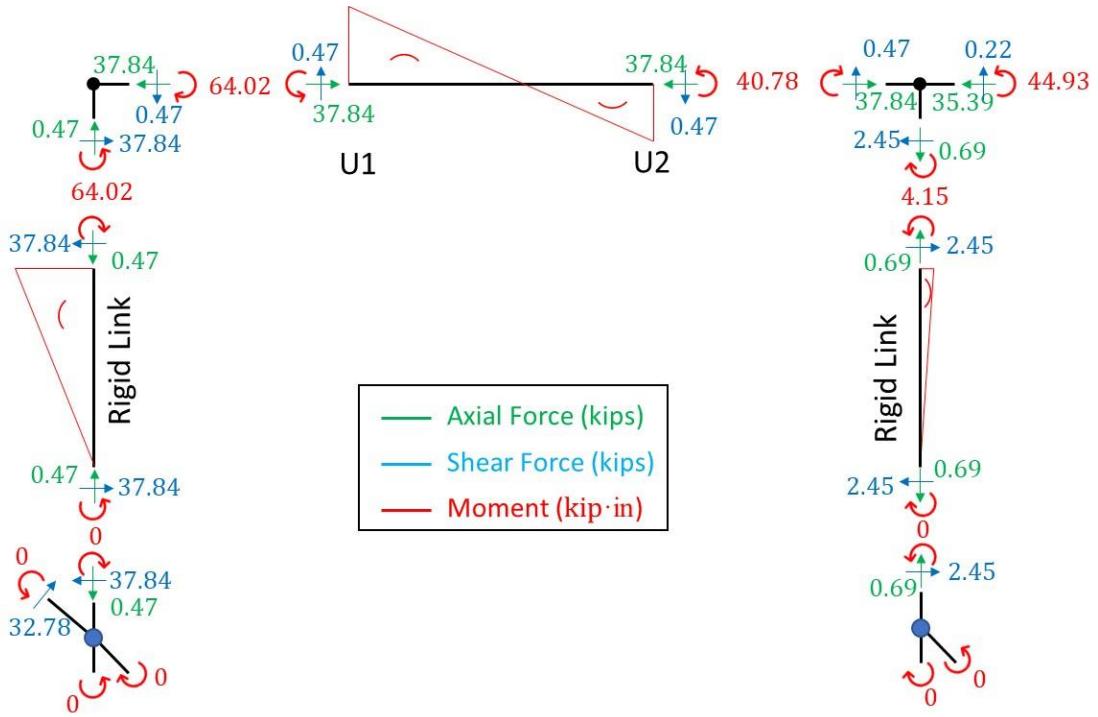
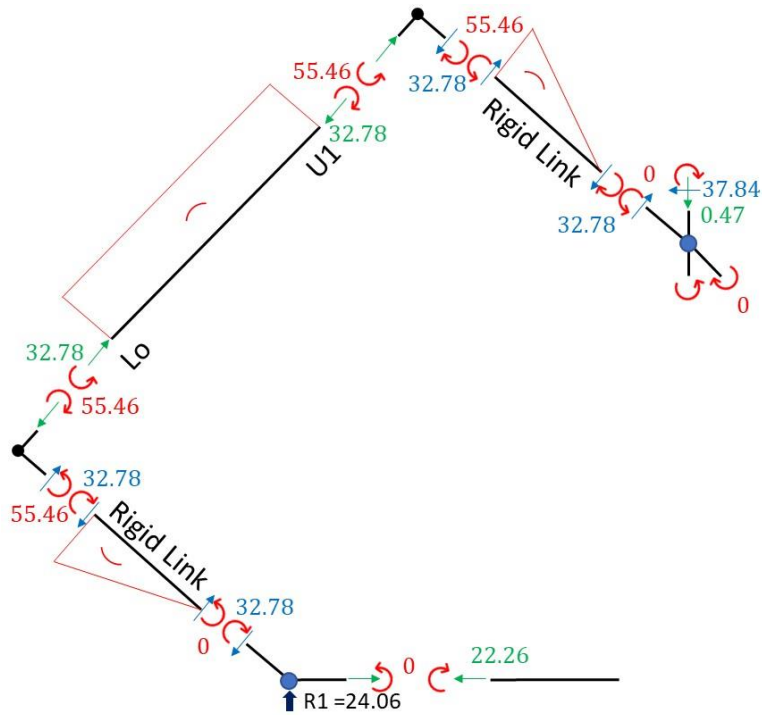


Figure 2.18 SAP2000 Analysis Results: Member Shear Forces

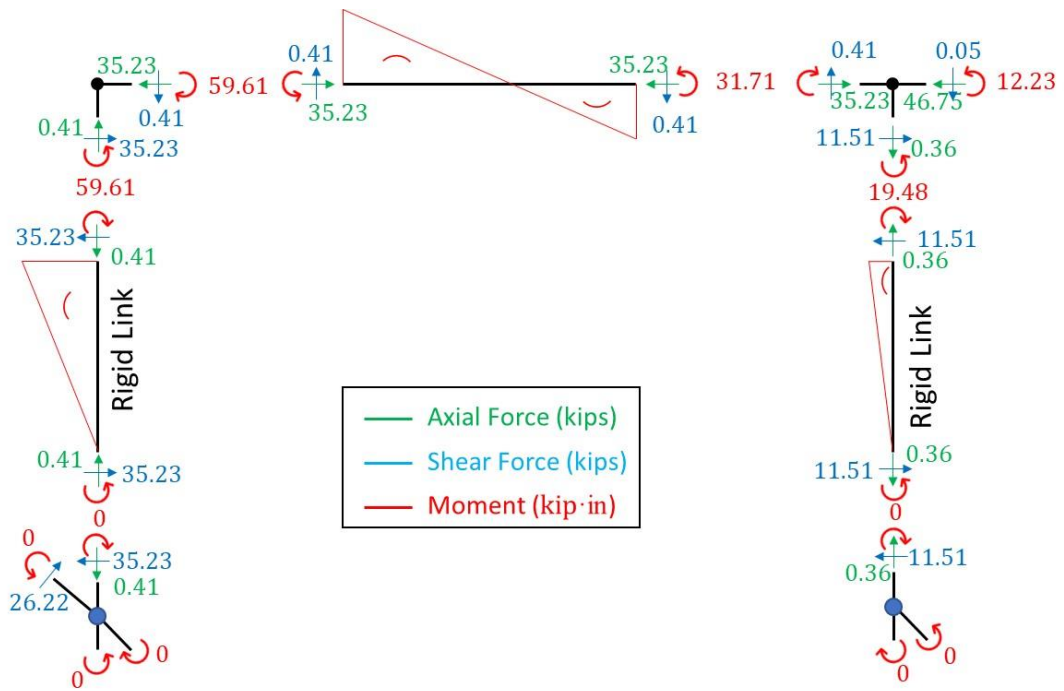


(a) Member U1U2

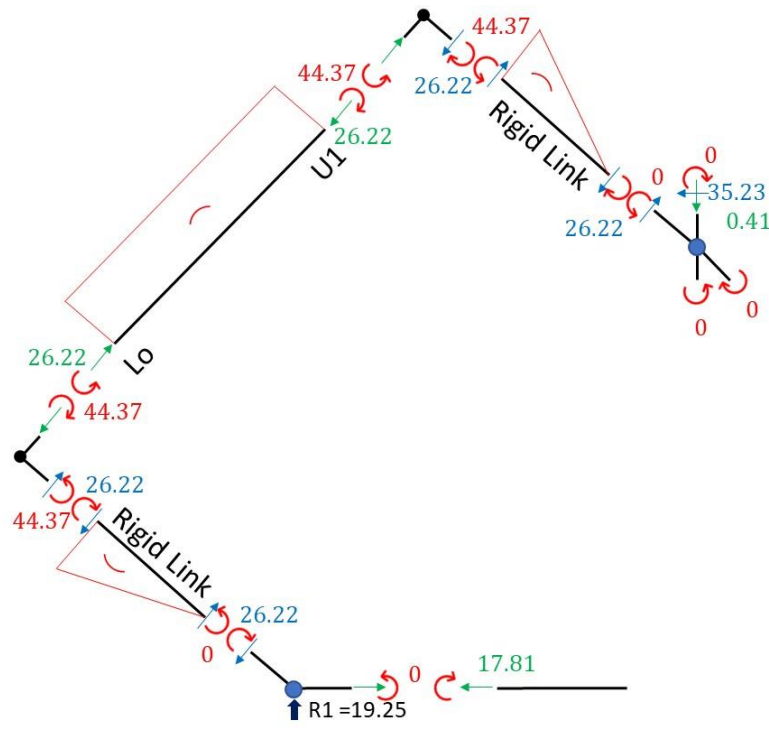


(b) Member L0U1

Figure 2.19 SAP2000 Analysis Results: Internal Forces of Members L0U1 and U1U2  
(Load Case 1)

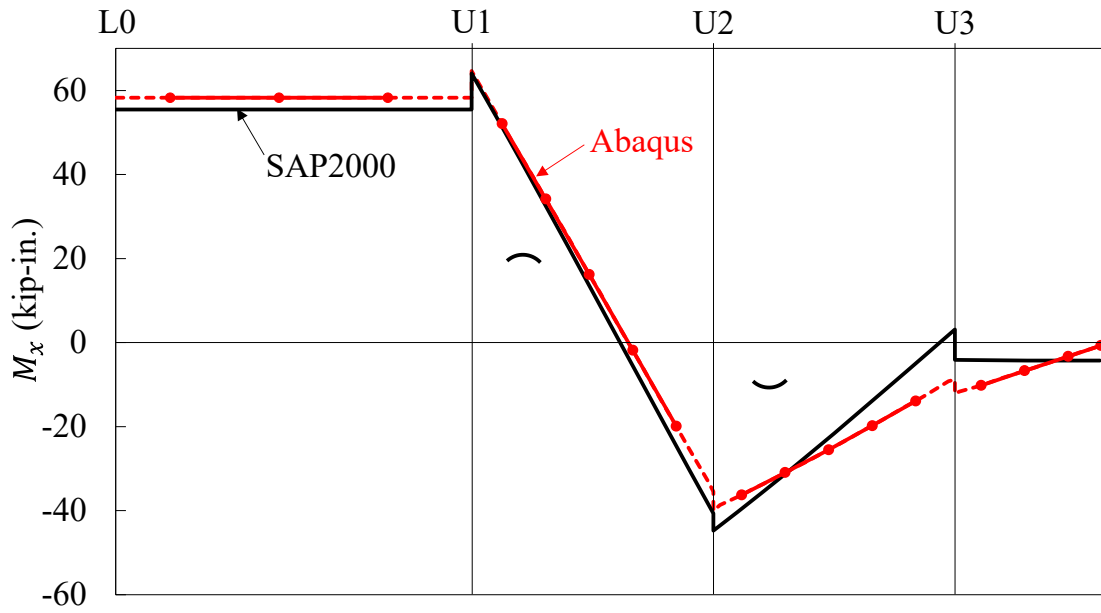


(a) Member U1U2

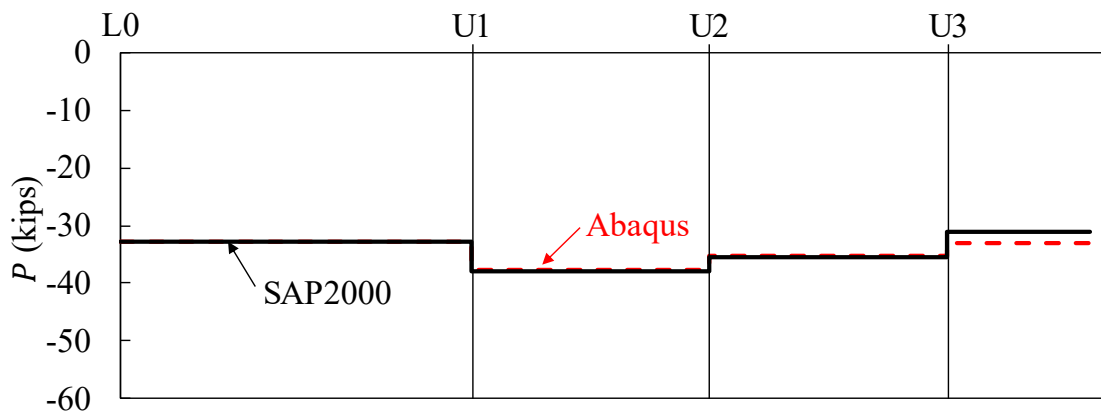


(b) Member L0U1

Figure 2.20 SAP2000 Analysis Results: Internal Forces of Members L0U1 and U1U2 (Load Case 2)

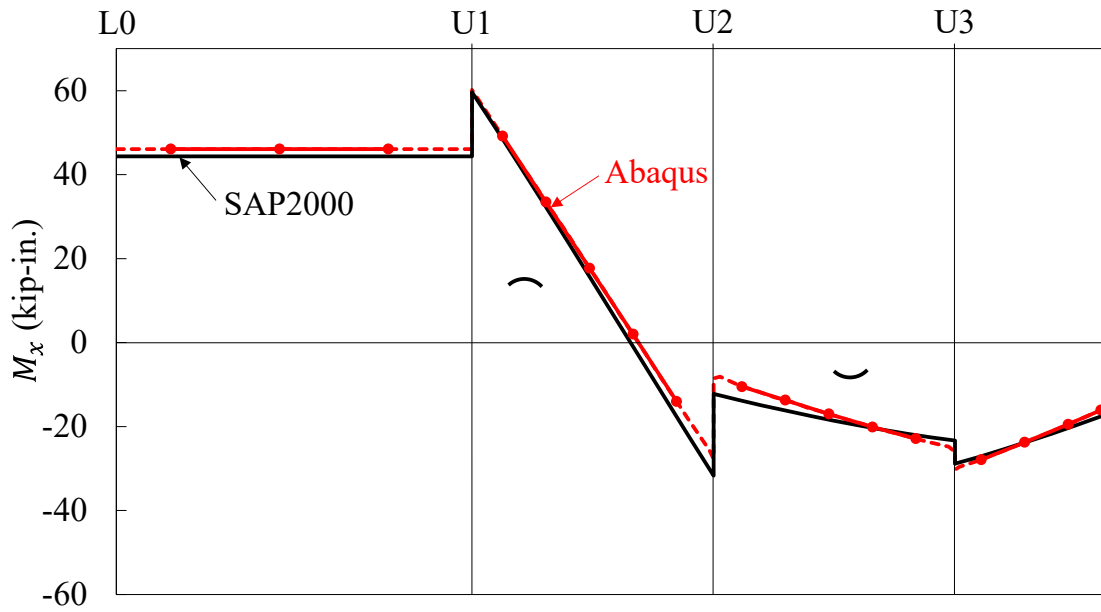


(a) Moment

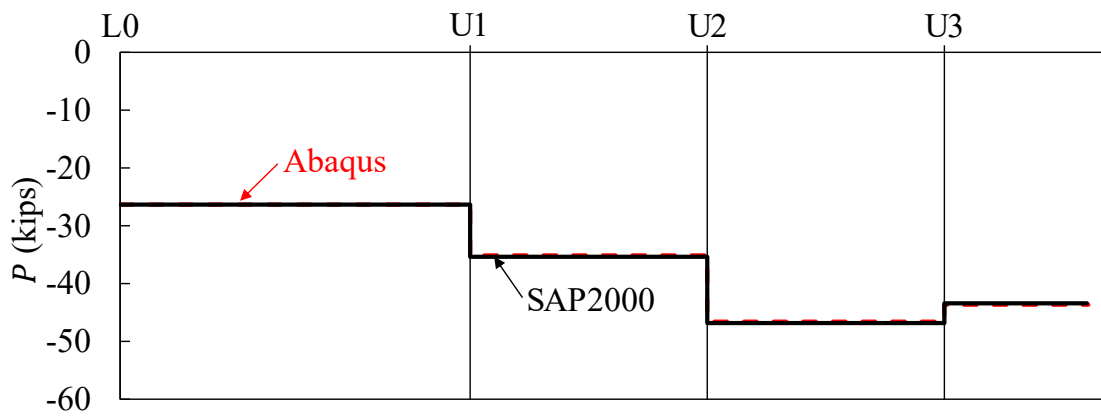


(b) Axial Force

Figure 2.21 Distribution of Moment and Axial Force (Load Case 1)

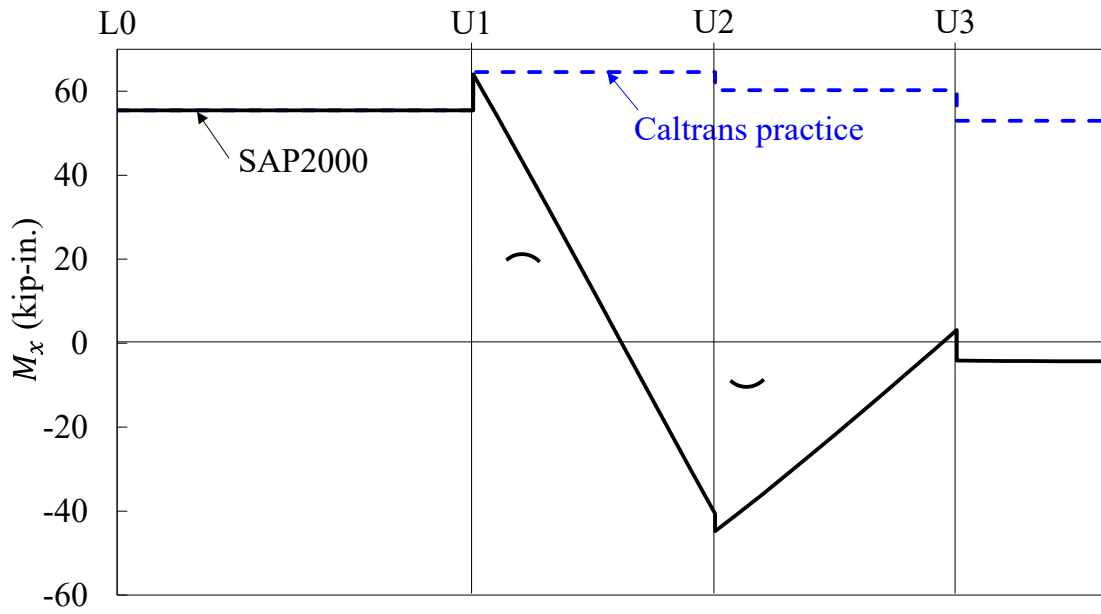


(a) Moment

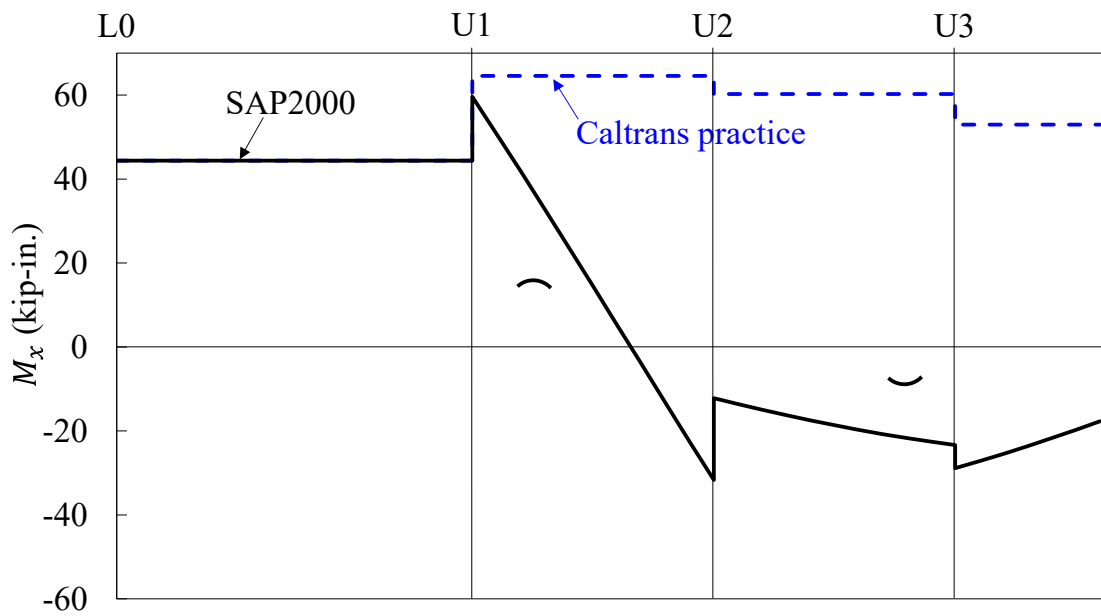


(b) Axial Force

Figure 2.22 Distribution of Moment and Axial Force (Load Case 2)

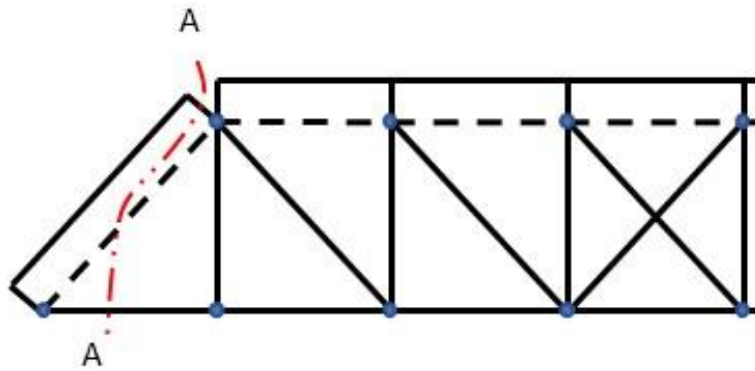


(a) Load Case 1

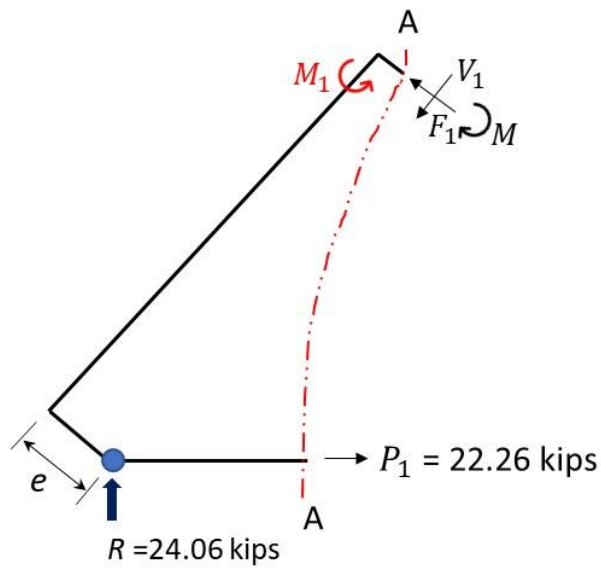


(b) Load Case 2

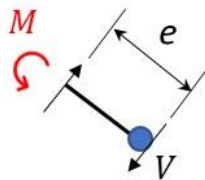
Figure 2.23 Comparison of Moments Based on SAP2000 and Caltrans Practice



(a) Section Cut A-A

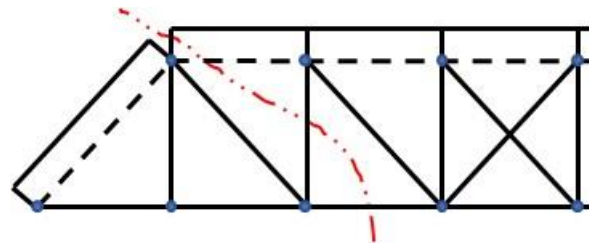


(b) Free-body Diagram for Determining Rigid Link Shear

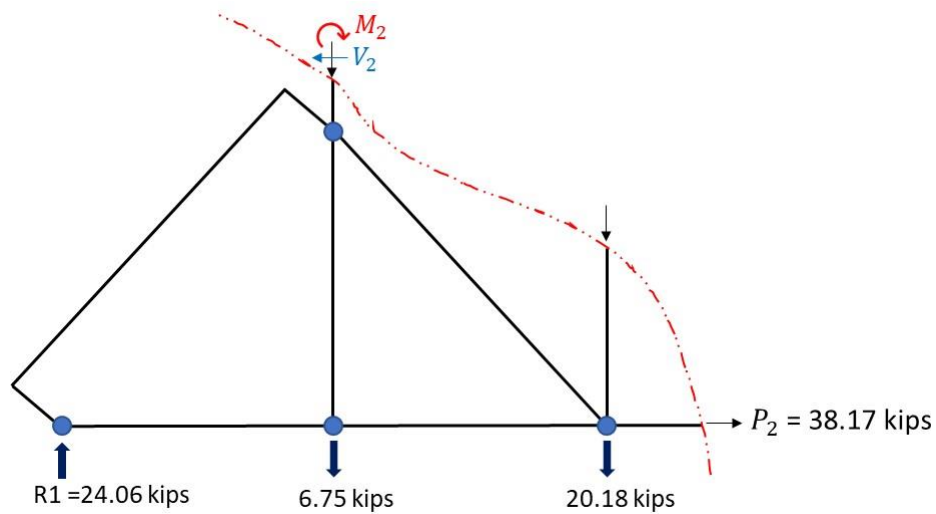


(c) End Moment

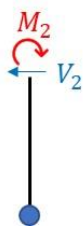
Figure 2.24 Determination of End Post Moment by Statics (Load Case 1)



(a) Section Cut



(b) Free-body Diagram for Determining Rigid Link Shear



(c) End Moment

Figure 2.25 Determination of Member U1U2 Moment by Statics (Load Case 1)

### **3 BRIDGE ROAD OVER SANTA PAULA CREEK: FIELD TESTING**

#### **3.1 General**

To verify the finite element analysis results presented in Chapter 2, field testing of the Bridge Road over Santa Paula Creek was conducted on June 17, 2019. A total of 20 staff members from UCSD and Caltrans participated in this testing. Caltrans assisted in traffic control, structural surface preparation for instrumentation, and loading the bridge with a water truck. UCSD staff were in charge of strain gauge instrumentation and data recording.

#### **3.2 Instrumentation**

Only one truss at westbound was instrumented with uniaxial strain gages. Three strain gages arranged as shown in Figure 3.2(a) were installed at 10 locations (Sections A-A to J-J in Figure 3.1). The figures also show that two strain gages were installed on two diagonal members at two locations (Sections K-K and L-L) to measure the axial strains in members U1L2, U2L3. The total number of strain gages used was 34. Figure 3.3 shows the preparation of the surface for installing strain gages, which involved grinding the painted surface to expose the metal first. The grinded surfaces were repainted at the conclusion of testing. Figure 3.4 shows the data acquisition system for recording the measured data. The bridge deflection along the span was recorded before and after loading by the UCSD survey crew.

It should be noted that the recorded responses were produced by the imposed water truck loading only; these measurements did not include components due to dead loads of the bridge.

#### **3.3 Loading Condition**

A water truck was used to apply loading to the bridge [Figure 3.5 (a)]; the weight of fore axle is 15.1 kips and the weight of rear axle is 34.4 kips, for a total weight of 49.5 kips. Figure 3.5(b) shows that the truck was positioned to be closer to the instrumented truss. Figure 3.6 shows the location of the truck along the span of the bridge for two load cases. For each load case, the truck drove slowly on the bridge and stopped at the marked location. The truck was positioned transversely as shown in Figure 3.5(b) to be closer to the

instrumented truss such that 68% of the total truck weight was resisted by the truss of interest.

### 3.4 Data Reduction

Figure 3.7 and Figure 3.8 show the measured data from field testing. For those sections that were instrumented with three strain gages [see Figure 3.2(a) for the gage designation], the axial force ( $P$ ), in-plane bending moment ( $M_x$ ), and out-of-plane bending moment ( $M_y$ ) are related to the recorded strains as follows:

$$E\epsilon_1 = \sigma_1 = \frac{P}{A} + \frac{M_x}{S_{xt}} + \frac{M_y}{S_{yt}} \quad (3.1)$$

$$E\epsilon_2 = \sigma_2 = \frac{P}{A} + \frac{M_x}{S_{xt}} - \frac{M_y}{S_{yt}} \quad (3.2)$$

$$E\epsilon_3 = \sigma_3 = \frac{P}{A} - \frac{M_x}{S_{xb}} - \frac{M_y}{S_{yb}} \quad (3.3)$$

where  $E$  is the elastic section modulus,  $S_{xb}$  and  $S_{yb}$  are the elastic section moduli with respect to  $\epsilon_3$ , respectively. Given the measured strains ( $\epsilon_1$ ,  $\epsilon_2$ ,  $\epsilon_3$ ), internal forces  $P$ ,  $M_x$ , and  $M_y$  then can be determined by solving the above simultaneous equations. Axial force is positive for tension, in-plane moment is positive when  $\epsilon_3$  is in compression, and out-of-plane moment is positive when  $\epsilon_3$  is in compression.

For the two diagonal members that were instrumented with two strain gages [see Figure 3.2(b)], the axial force is computed as

$$P = \frac{(\epsilon_1 + \epsilon_2)}{2} \cdot (2A) \cdot E \quad (3.4)$$

where  $A$  (2.43 in<sup>2</sup> and 1.56 in<sup>2</sup> for the sections K-K and L-L, respectively) is the cross-sectional area of one of the pair of bars for each diagonal member.

### 3.5 Results of Field Testing

Table 3.1 summarizes the calculated moments and axial forces from field testing. A graphic representation of these experimentally determined internal forces along the bridge span for both load cases are shown in Figure 3.9 and Figure 3.10, respectively. Minor flexural bending in the out-of-plane is noted because the truss is not perfectly planar as is

commonly assumed in the analysis. Measured vertical deflections of the truss are presented in Table 3.2 and Figure 3.11.

### 3.6 Correlation Study

Measured responses are compared with those from finite element analyses in this section. Figure 3.12 shows that the measured vertical deflection profiles correlate very well with the predictions by finite element analyses.

A comparison of the experimentally determined member forces with those from finite element predictions are presented in Figure 3.13 and Figure 3.14. It is observed that the axial forces determined from field tests are consistently lower than the predictions by about 10%. The moment diagrams from both testing and finite element analyses are also consistent, capturing the trend in bending direction (e.g., double curvature in member U1U2, single curvature in members L0U1 and U2U3). The correlation is reasonable considering the uncertainties in testing (e.g., truck load magnitude and location) and analyses (e.g., frictionless pins assumed in finite element analyses.)

Based on the test data, it is possible to evaluate the effect of rotational friction to the member end moment. Consider member U1U2 in Load Case 1 for example, the average axial force from Table 3.1 is 33.2 kips. If the pin at joint U1 is assumed to be frictionless, the expected end moment is 56.2 kip-in ( $= P e = 33.2 \times 1.692$ ) based on statics [see Figure 3.15(a)]. Next, extrapolating the experimentally determined end moment diagram of member U1U2 to joint U1 gives an end moment of 47 kip-in, which is smaller than 56.2 kip-in due to the friction effect in the pin. Referring to the free-body diagrams in Figure 3.15(b), the frictional moment,  $M_f$ , equals

$$M_f = P e - 47 = 9.2 \text{ kip-in} \quad (3.5)$$

Therefore, 16% of the expected end moment ( $= 56.2 \text{ kip-in}$ ) is resisted by the frictional moment in the pin.

Table 3.1 Moment and Axial Force from Field Testing

Member	Location (in.)	Load Case 1			Load Case 2		
		$M_x$ (kip-in.)	$M_y$ (kip-in.)	$P$ (kips)	$M_x$ (kip-in.)	$M_y$ (kip-in.)	$P$ (kips)
L0U1	88	19.1	-23.4	-38.7	10.5	-21.7	-23.9
	169	23.3	17.0	-28.6	18.0	20.6	-22.4
	294	26.2	7.5	-30.1	22.0	17.1	-21.6
U1U2	359	-36.5	-4.3	-34.0	-38.2	1.1	-30.6
	434	-12.8	-0.9	-32.4	-18.0	1.1	-28.7
	517	17.3	-2.7	-33.1	10.0	-7.2	-28.4
U2U3	689	22.0	1.1	-30.4	10.0	-1.0	-38.6
	661	14.7	5.8	-30.9	15.1	5.8	-39.9
	728	4.9	0.8	-31.1	18.6	1.2	-40.7
U3U4	808	14.1	-4.4	-27.7	28.4	-2.7	-37.5

Table 3.2 Vertical Deflection of Bridge from Field Tests

Location (in.)	Load Case 1 (in.)	Load Case 2 (in.)
0	0.00	0.00
222	-0.24	-0.16
444	-0.39	-0.35
666	-0.39	-0.59
888	-0.28	-0.43
1110	-0.20	-0.20
1332	-0.12	-0.12
1554	0.00	0.00

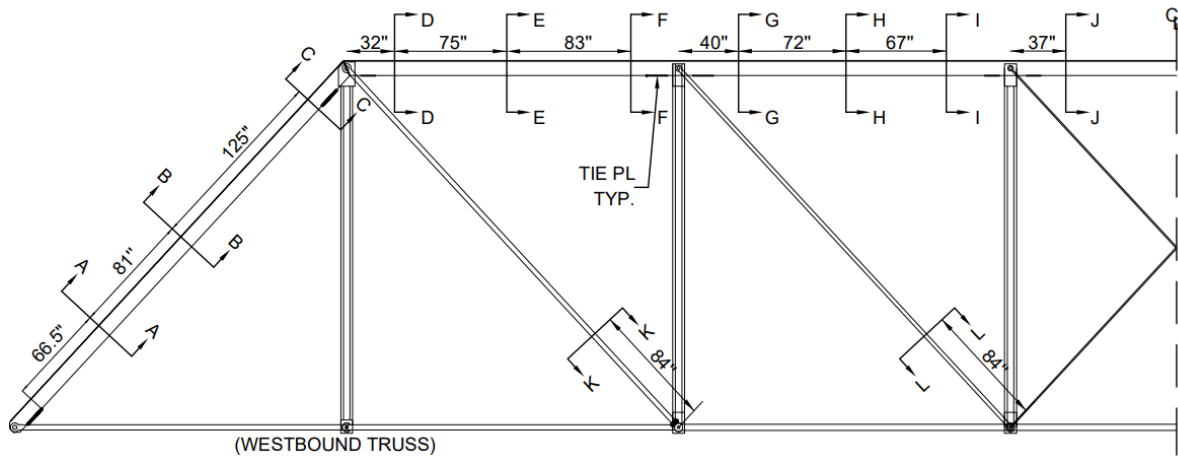


Figure 3.1 Instrumentation Elevation

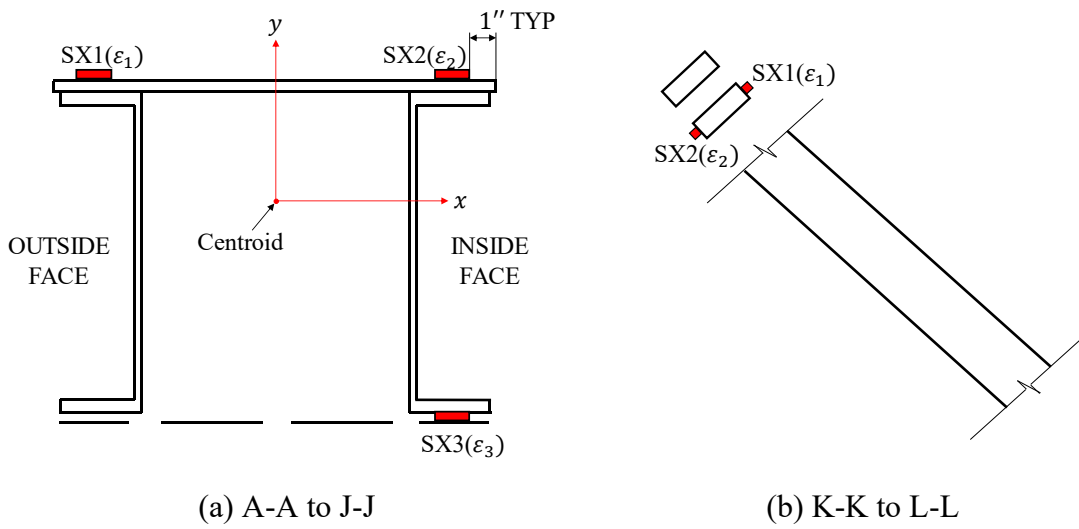


Figure 3.2 Instrumentation Section



Figure 3.3 Surface Preparation



Figure 3.4 Data Acquisition System

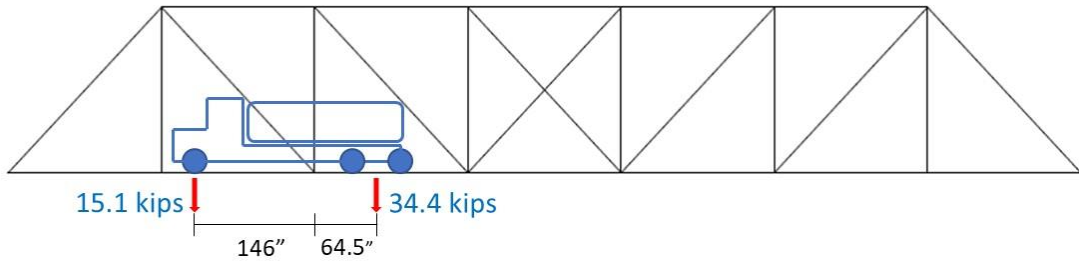


(a) Water Truck

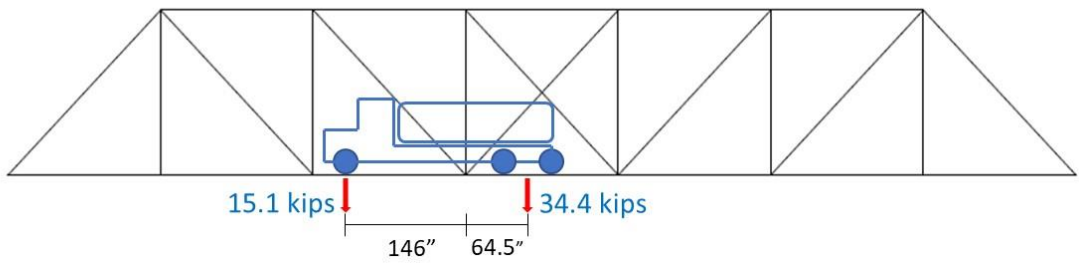


(b) Positioning of Water Truck for Load Test

Figure 3.5 Water Truck for Load Tests



(a) Load Case 1



(b) Load Case 2

Figure 3.6 Truck Loading for Field Tests

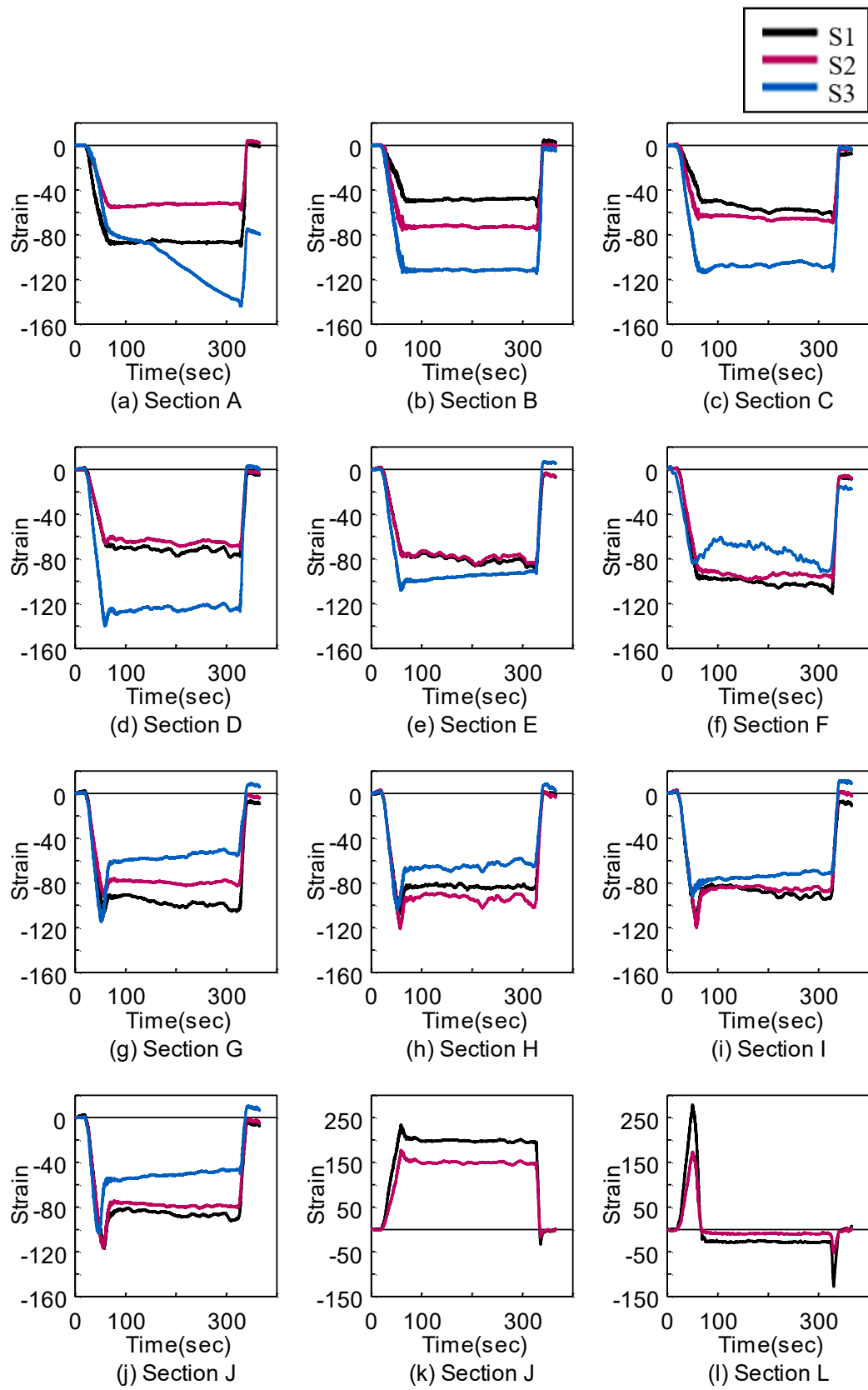


Figure 3.7 Recorded Strain Gage Data (Load Case 1)

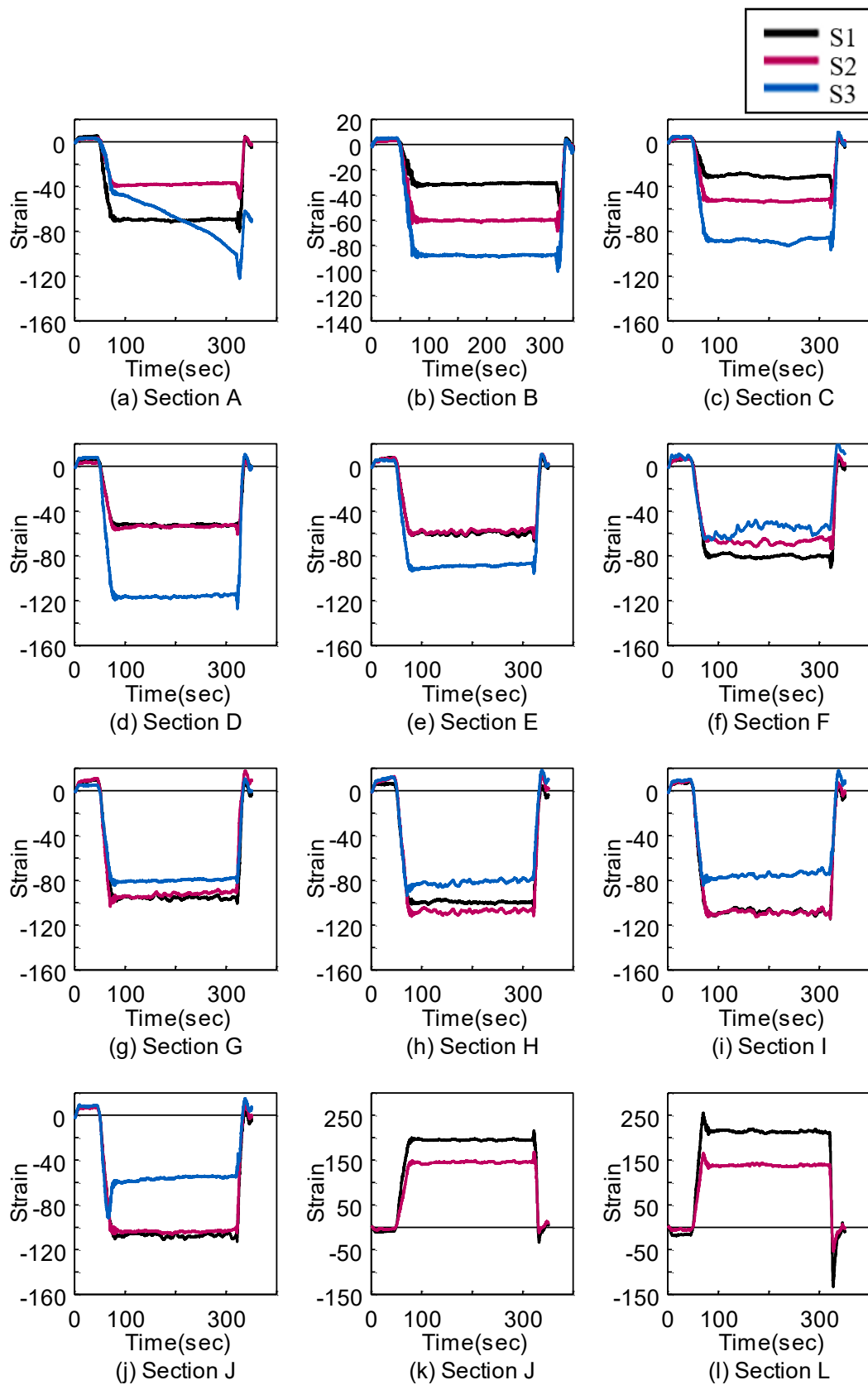
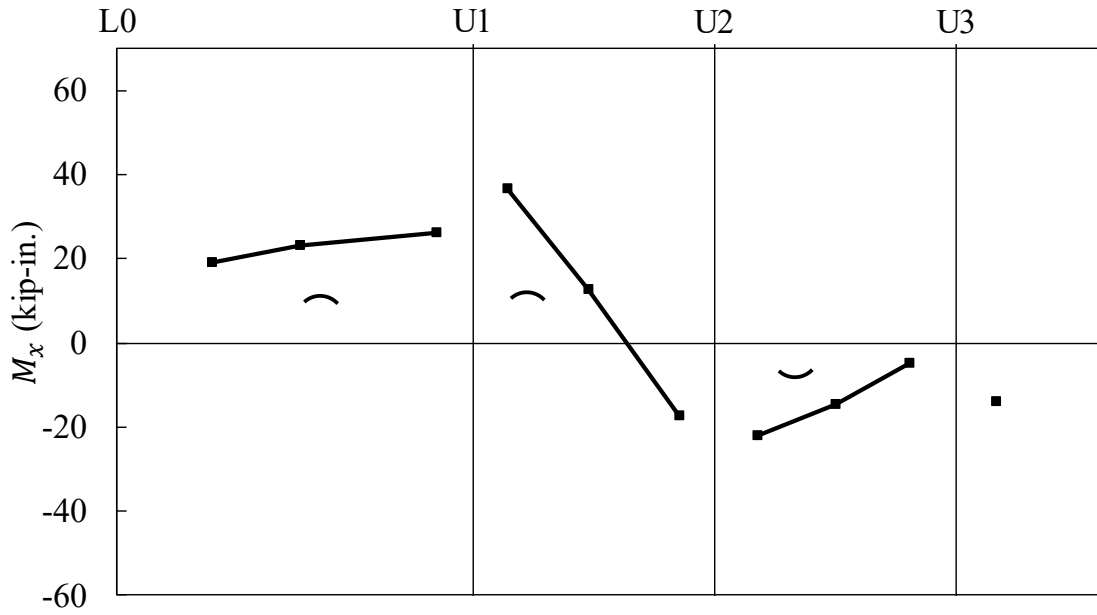
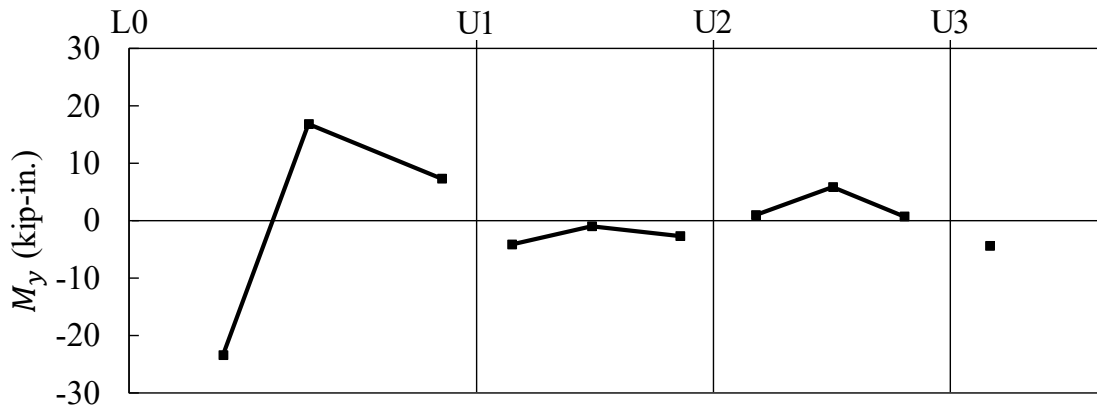


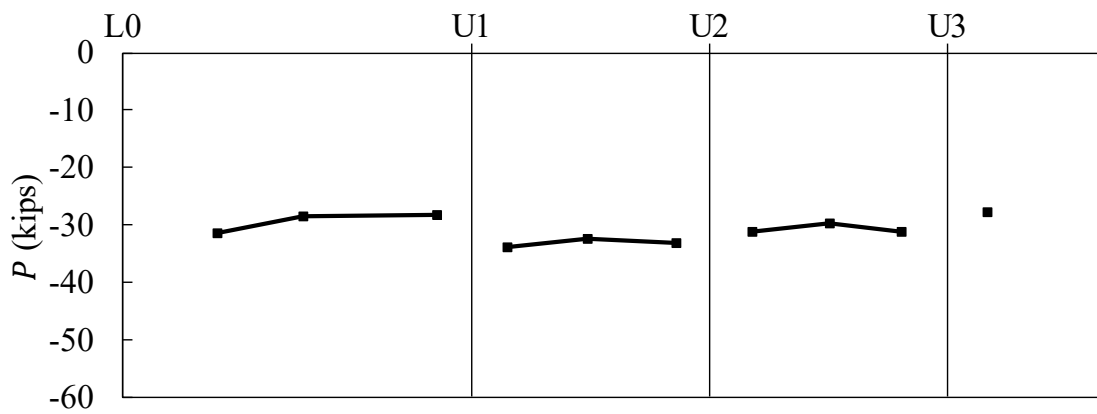
Figure 3.8 Recorded Strain Gage Data (Load Case 2)



(a) Moment about X-axis

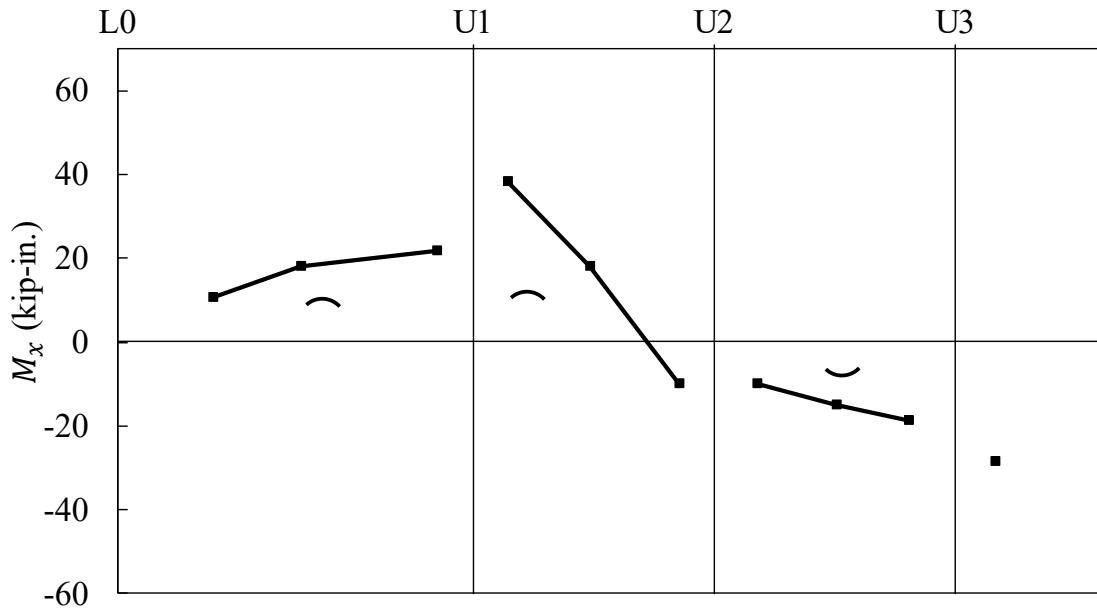


(b) Moment about Y-axis

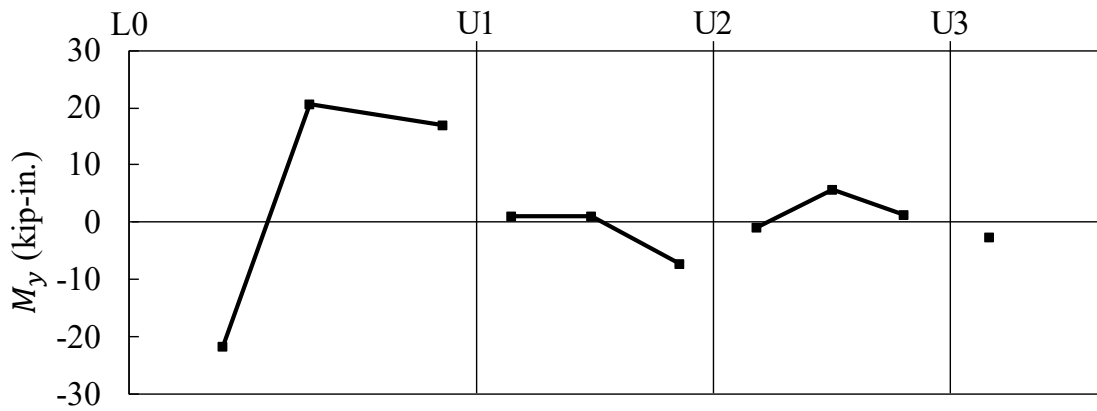


(c) Axial Force

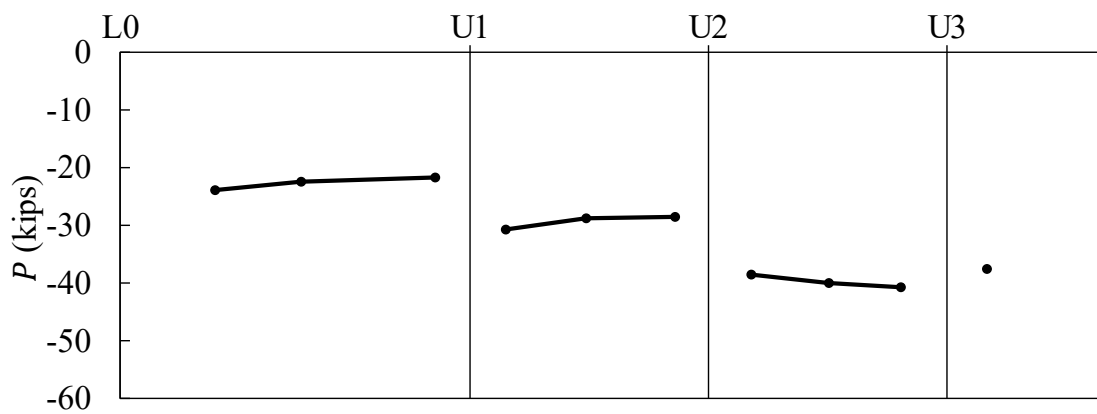
Figure 3.9 Distribution of Moment and Axial Force from Field Testing (Load Case 1)



(a) Moment about X-axis

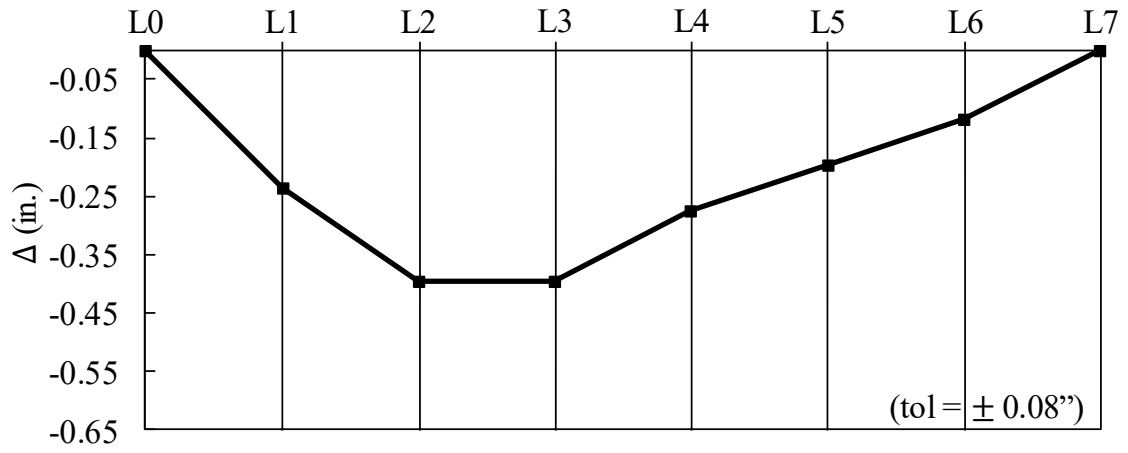


(b) Moment about Y-axis

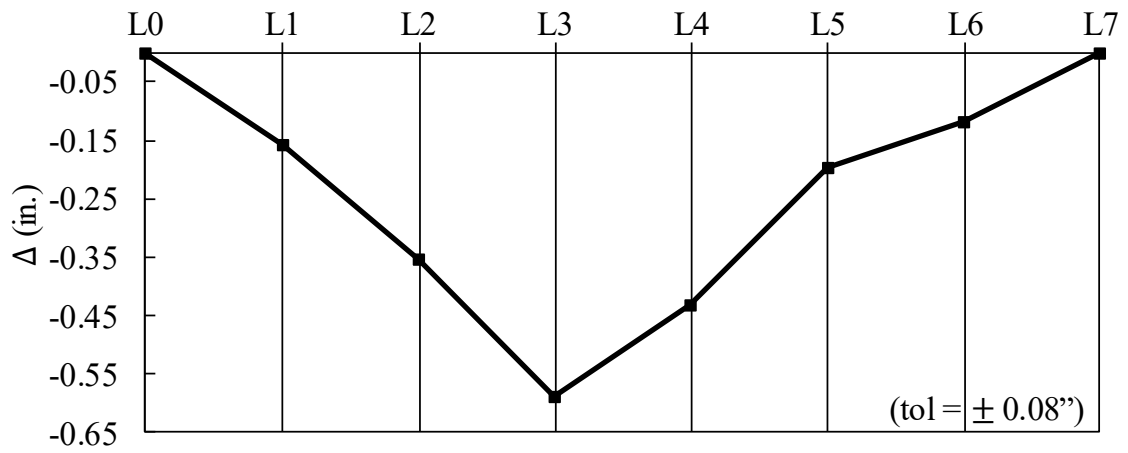


(c) Axial Force

Figure 3.10 Distribution of Moment and Axial Force from Field Testing (Load Case 2)

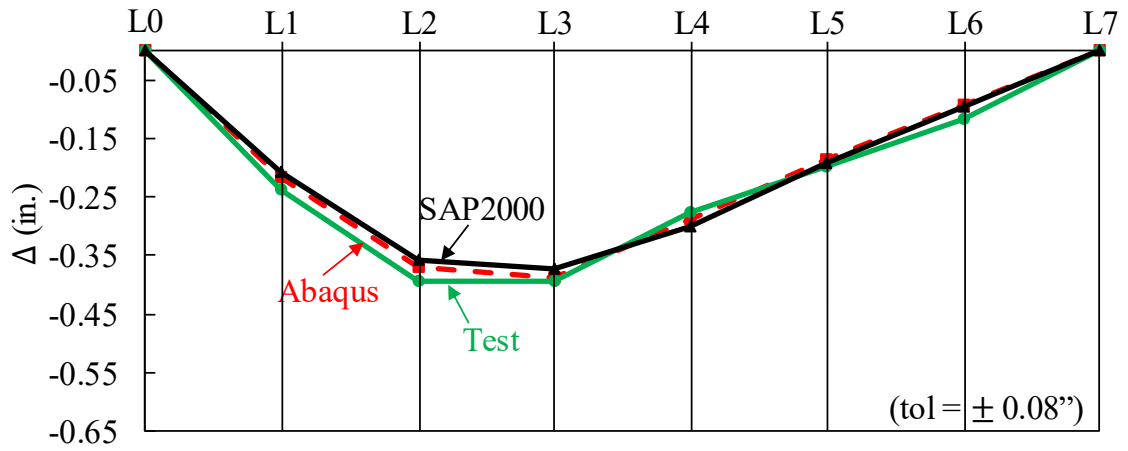


(a) Load Case 1

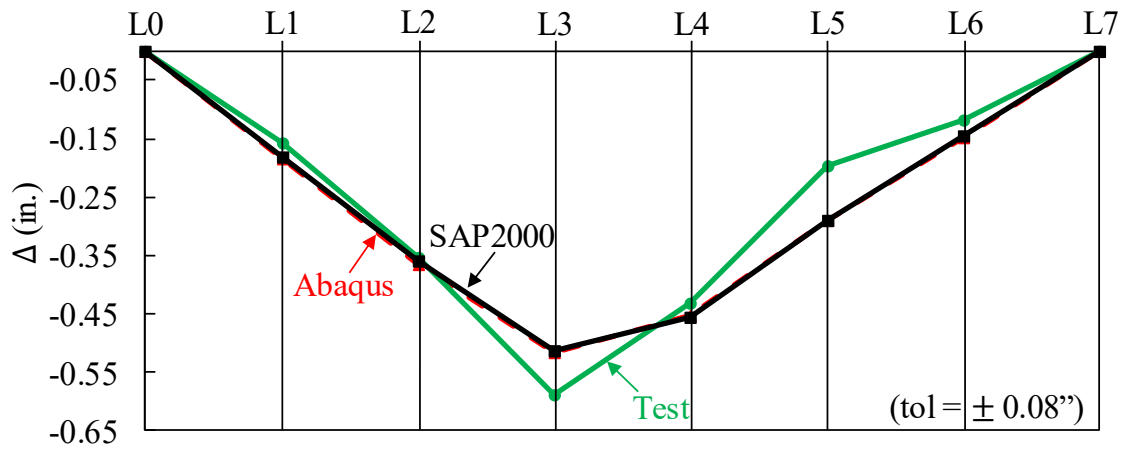


(b) Load Case 2

Figure 3.11 Vertical Deflection of Truss from Field Testing

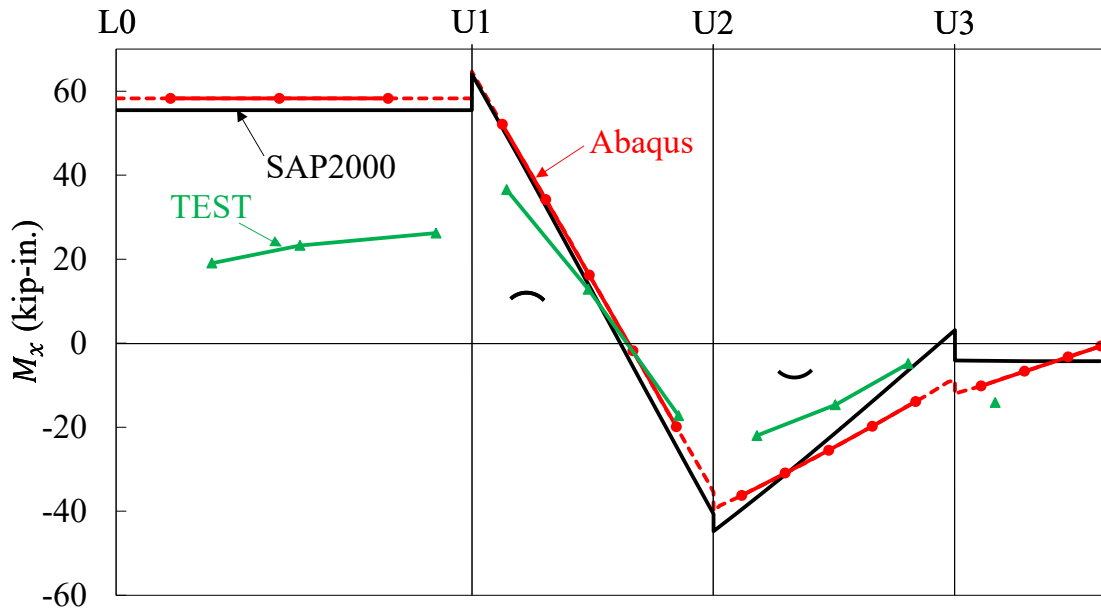


(a) Load Case 1

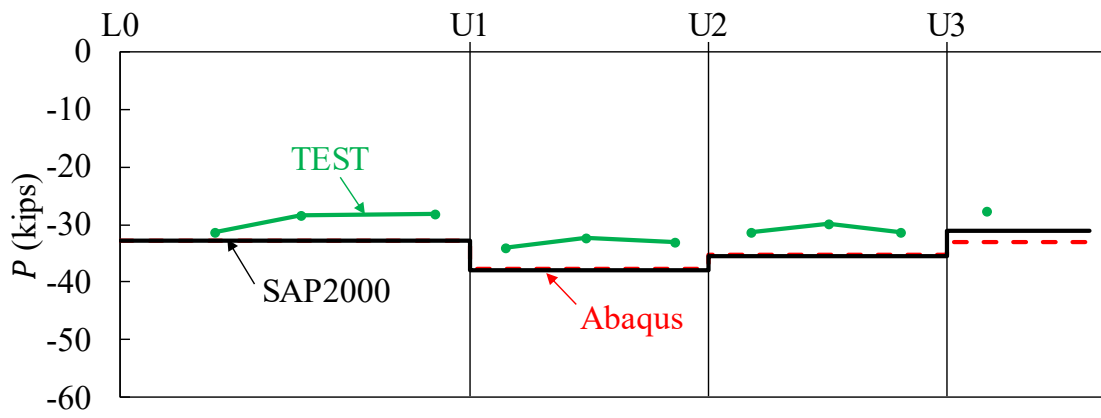


(b) Load Case 2

Figure 3.12 Comparison of Vertical Deflections

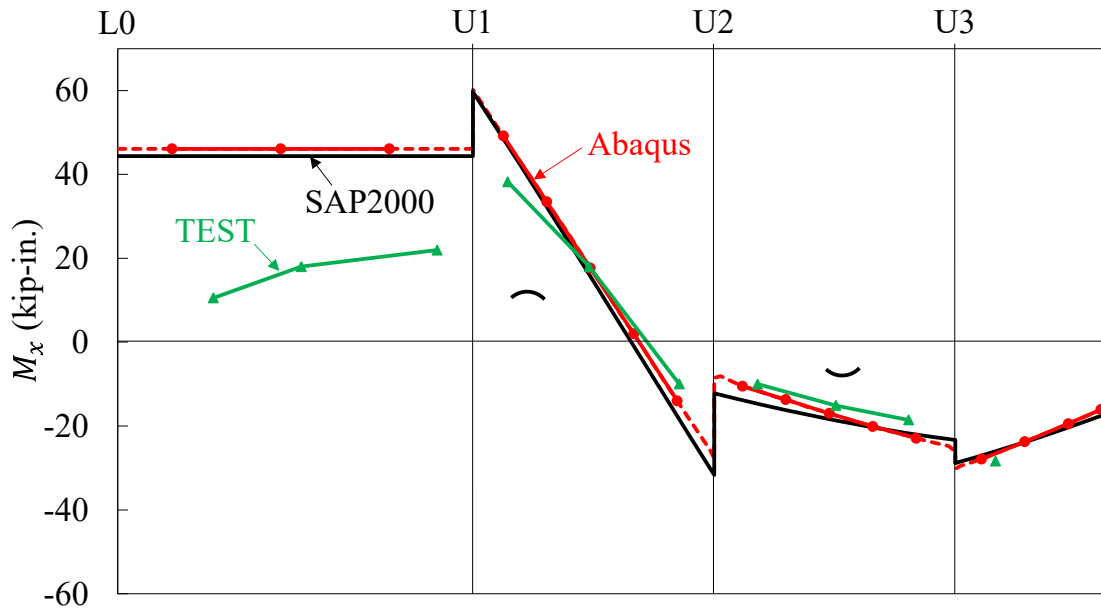


(a) Moment about X-axis

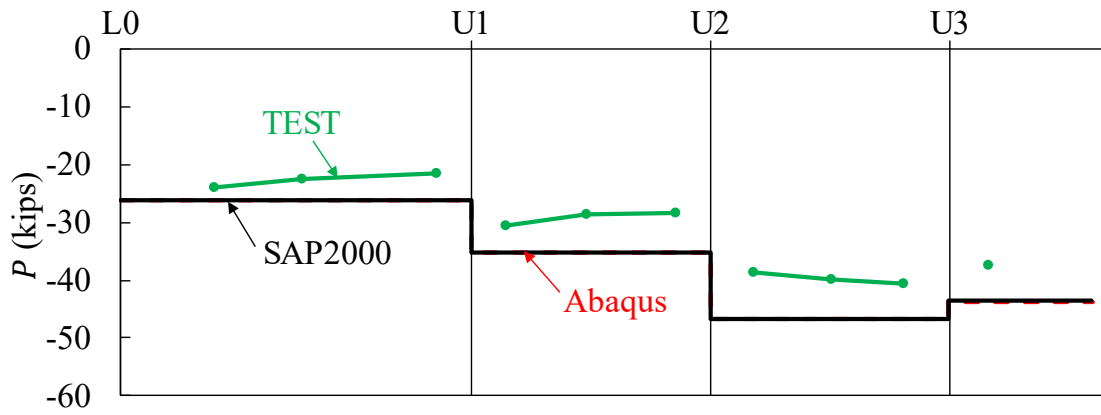


(b) Axial Force

Figure 3.13 Comparison of Moments and Axial Forces (Load Case 1)

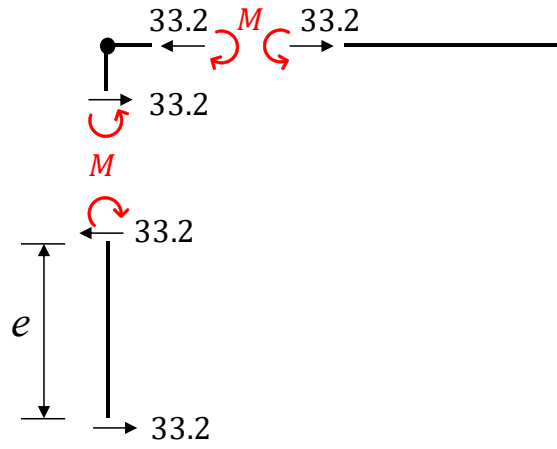


(a) Moment about X-axis

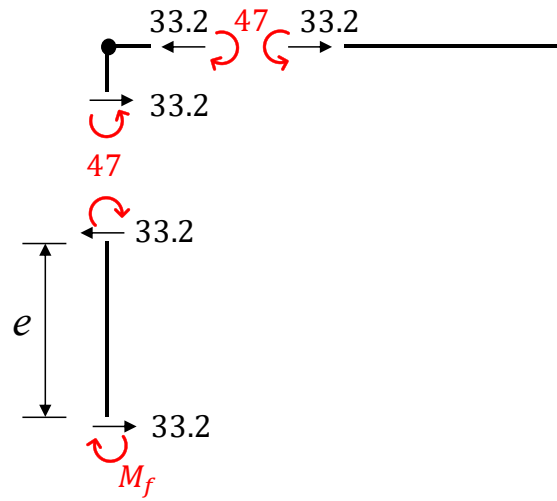


(b) Axial Force

Figure 3.14 Comparison of Moments and Axial Forces (Load Case 2)



(a) Frictionless Pin Assumption



(c) Pin with Friction

Figure 3.15 Effect of Friction in Pin Joint U1 (Load Case 1)

## 4 BRIDGE ROAD OVER KLAMATH RIVER

### 4.1 General

The 190-ft long Bridge Road over Klamath River (Structure No. 020119), located in Siskiyou County, California is a typical through Parker truss bridge that was constructed in 1954. The bridge features built-up members interconnected by riveted gussets at joints of the truss. According to the as-built repair plan dated in 1986, the lacing plates at the bottom of top chords and end posts were replaced by continuous plates between truss panel points. No field testing was conducted on this bridge. This chapter presents the results from finite element analysis. The repaired truss bridge was first analyzed, which was then followed by the original truss bridge in Section 4.6.

### 4.2 Description of Bridge

Figure 4.1 shows the bridge in its existing condition; it was rated as Good by Caltrans in 2018. Figure 4.2 depicts the elevation and overall dimensions of the truss. The cross section of the bridge is shown in Figure 4.3. The bridge features concrete deck, stringers (WF24×76, 21 total), WF36×160 floor beams. ASTM A7 steel was specified for the trusses. Figure 4.4 shows the as-built drawing of the bridge truss.

The cross section of each truss member is summarized in Table 4.1. All members are connected by riveted gussets (see Figure 4.5 for a sample joint). Pins are used at the supports. Cross sectional dimensions of four types of built-up members used in this bridge are summarized in Figure 4.6. According to the as-built design drawing in Figure 4.4, the working line is 2.0 in. above the mid-depth of the double-channel of the top chord. The distance from the centroid to the working line (i.e., eccentricity,  $e$ ) is provided in Table 4.1. Due to the different thicknesses of the cover plates at the top and bottom faces, the upper chord members have different eccentricities. Also note the working lines at the supports do not meet at the pin connection.

### 4.3 Abaqus Analysis

Four-node quadrilateral shell element (S4R) with reduced integration was used to model all the members and connecting plates. Each rivet was also modeled by using the

point-based “Fastener” in Abaqus. Models at selected joints are shown in Figure 4.7 and Figure 4.8.

Two load cases were considered (see Figure 4.9). Load Case 1 has a concentrated load of 100 kips applied at the midspan to maximize the compressive axial force in the top chord U3U4. Load Case 2 has two concentrated loads of 50 kips each and the loads are applied to maximize the compressive axial force in the end post L0U1. Figure 4.10 shows the deflections of the truss for both load cases. Figure 4.11 and Figure 4.12 show the axial force and moment distributions along the compressive chord of the truss. In these figures, solid dots in the moment diagram represent locations along the member length that moments were calculated from stresses along the depth of the cut sections. These sections were selected between end gusset regions, i.e., sections were not chosen in the gusset region to avoid a complicated stress state. The dash-line portions of the moment diagram, also shown in red, were extrapolated from the solid-line portions such that member end moments at joints (e.g., U1) could be determined. The axial forces and extrapolated member end moments are summarized in Table 4.2.

## **4.4 SAP2000 Analysis**

### **4.4.1 General**

In order to evaluate if commonly used computer software with simple truss or beam elements can reliably predict the “actual” internal member forces, especially moments, from Abaqus, structural analysis using SAP2000 was performed.

### **4.4.2 Model 1**

The geometry of the truss model was based on the working line (see Figure 4.13). Two models were created, one with pin joints and one with rigid joints. As expected, the member axial forces are very similar. Therefore, only results from the latter model are presented. The predicted vertical deflections of the truss (Figure 4.10) and member axial forces [Figure 4.11(b) and Figure 4.12(b)] correlate very well with those from Abaqus. Moment diagrams of the top chord for both load cases are compared in Figure 4.11(a) and Figure 4.12(a). The general observation is that the correlation of the moment diagram is poor, particular for member L0U1.

### 4.4.3 Model 2

The geometry of Model 1 was based on working lines. Since Model 1 cannot predict member moments well, a second model was constructed. In this case, centroidal lines of truss member were used to define the geometry. As a result, eccentricity exists in all joints of the top chord; see Figure 4.14. Taking joint U1 for example, two nodes are specified in the SAP2000 model. One node is specified for two intersecting chord members (L0U1 and U1U2), and another node is specified for the other two intersecting members (vertical L1U1 and diagonal L2U1). Since all four members are connected by a gusset plate, a rigid link of a length 2.24 in. was used to connect these two nodes. A rigid link was also used at support L0 because the centroidal axes of two connected members do not intersect at the center of the pin.

The moment diagrams produced from Model 2 are also added to Figure 4.11(a) and Figure 4.12(a). Recall that member L0U1 shows the largest discrepancy between Abaqus and Model 1 moment results. But the correlation for both load cases is excellent with the use of Model 2. The improvement in the moment diagram correlation is also obvious for member U2U3 (Load Case 1) and member U1U2 (Load Case 2).

To provide an insight into the actual behavior, first consider joint U1 (see Figure 4.15). Four members are connected by a gusset connection at this location; the centroidal axes of top chords L0U1 and U1U2 meet at point “A” in the figure, and the centroidal axes of vertical L1U1 and diagonal L2U1 meet at point “B.” Taking Load Case 1 for example, the shear (= 14.52 kips) in the rigid link that connects points “A” and “B” produces an end moment of 27.57 kip-in. (counterclockwise) at end “B.” This moment is balanced by an end moment of 43.80 kip-in. (clockwise) in chord L0U1 and an end moment of 16.23 kip-in. (counterclockwise) in chord L1L2. At the other end of the rigid link, the 4.94 kip-in. counterclockwise moment is balanced by the end moments of vertical L1U1 (1.90 kip-in.) and diagonal L2U1 (3.04 kip-in.), both in the clockwise direction. A similar presentation of joint U3 is presented in Figure 4.16.

Figure 4.17 shows the free-body diagrams at support L0. Centroidal axes of end post L0U1 and bottom chord L0L1 intersect at point “B,” which does not coincide with the center of the pin at “A” (see Figure 4.4). The shear (= 65.84 kips) in the 3.41-in. long rigid

link produces an end moment of 224.33 kip-in, and 92% of which (= 206.08 kip-in.) is resisted by the bottom end of end post L0U1.

#### **4.5 Caltrans Practice**

Following the Caltrans practice to ignore the end eccentricity in a truss analysis and then multiply the member axial forces by 50% of the end eccentricity to compute member end moments for truss with riveted or bolted gusset connection, the moment diagrams of the top chord are presented in Figure 4.18 for comparison with moment diagrams produced by both Abaqus and Model 2 of SAP2000. It was shown earlier that the latter two moment diagrams are consistent. Also note that the Caltrans procedure would predict a uniform bending (i.e., no moment gradient) in each chord member for this truss.

Refer to Load Case 1 in Figure 4.18(a) and consider member L0U1 first. The single-curvature, uniform moment diagram based on the Caltrans practice contradicts the actual double-curvature moment diagram. For members U1U2 and U2U3, the direction of the curvature based on the Caltrans practice is opposite that of the actual curvature. For member U3U4, the large moment gradient in the actual moment diagram cannot be predicted by the Caltrans practice; the Caltrans practice will also produce a moment magnifier,  $\delta_b$ , larger than 1.0, which is mostly likely unnecessary. In addition, the Caltrans practice under-predicts the magnitude of the largest moment by about 50% (132.3 kip-in. versus the actual moment of 270.5 kip-in.) Therefore, the Caltrans practice fails to predict the actual moment diagrams in the top chords.

#### **4.6 Effect of Retrofit**

According to the as-built repair plan dated in 1986, the bottom plates in the top chords and end posts were added (see Figure 4.6 and Table 4.1). An additional Abaqus analysis with Load Case 1 was conducted to evaluate the effect of this strengthening scheme. In the analysis, the bottom cover plates were removed to simulate the original condition of the truss.

The predicted moment and axial load diagrams are presented in Figure 4.19. As expected, the member axial forces are not affected. But Figure 4.19(a) shows that the moments, especially those in the end post and chord U3U4, are increased, indicating that the strengthening scheme actually increases the eccentricity in some members.

Table 4.1 Truss Member Sizes

Member Designation	Cross Section	Cross Section Type <sup>a</sup>	Eccentricity, <i>e</i> (in.)
L0U1, L8U7 (end posts)	2C15×50 + PL5/8×18 (Top) PL5/8×18 (Bot)	1	-2
U1U2, U7U6 (top chords)	2C15×33.9 + PL7/16×18 (Top) PL1/2×18 (Bot)	2	-2.238
U2U3, U6U5 (top chords)	2C15×40 + PL7/16×18 (Top) PL1/2×18 (Bot)	3	-2.218
U3U4, U5U4 (top chords)	2C10×40 + PL1/2×18 (Top) PL1/2×18 (Bot)	4	-2
L0 to L2, L6 to L8 (bottom chords)	2C15×33.9		-
L2L3, L5L6 (bottom chords)	2C15×40		-
L3L4, L4L5 (bottom chords)	2C15×50		-
All for diagonals and vertical members not listed the table	WF10×33		-

<sup>a</sup>See Figure 4.6.

Table 4.2 Moments and Axial Forces from Abaqus

Member	Location (in.)	Load Case 1		Load Case 2	
		$M_x$ (kip-in.)	$P$ (kips)	$M_x$ (kip-in.)	$P$ (kips)
LOU1	50	-98.8	-69.3	-195.4	-112.2
	200	-42.9		-141.2	
	350	13.2		84.0	
U1U2	450	15.6	-76.7	-44.1	-85.9
	550	24.4		-62.3	
	650	33.2		-80.7	
U2U3	750	10.2	-101.7	-50.6	-63.5
	850	12.5		-20.3	
	950	13.0		6.0	
U3U4	1050	-46.1	-133.3	31.1	-50.4
	1150	-150.5		2.6	
	1250	-249.2		-25.4	

Table 4.3 Moments and Axial Forces from SAP2000 (Model 1)

Member	Location (in.)	Load Case 1		Load Case 2	
		$M_x$ (kip-in.)	$P$ (kips)	$M_x$ (kip-in.)	$P$ (kips)
LOU1	0	-13.1	-68.7	-49.3	-111.0
	415.3	8.5		-94.0	
U1U2	415.3	14.6	-75.9	-97.3	-84.9
	715.5	44.6		-68.0	
U2U3	715.5	60.3	-100.7	-74.6	-62.9
	1002.2	-13.8		47.5	
U3U4	1002.2	5.6	-132.3	43.0	-49.9
	1287.2	-277.0		-19.3	

Table 4.4 Moments and Axial Forces from SAP2000 (Model 2)

Member	Location (in.)	Load Case 1		Load Case 2	
		$M_x$ (kip-in.)	$P$ (kips)	$M_x$ (kip-in.)	$P$ (kips)
LOU1	0	-112.5	-69.4	-206.1	-112.2
	415.3	43.8		-65.3	
U1U2	415.3	16.2	-76.7	-39.4	-85.8
	715.5	60.2		-98.5	
U2U3	715.5	25.7	-101.7	-62.0	-63.5
	1002.2	12.4		28.7	
U3U4	1002.2	-8.0	-133.3	56.1	-50.4
	1287.2	-270.5		-20.5	

Table 4.5 Vertical Deflection of Bridge

Joint No.	Load Case 1			Load Case 2		
	Abaqus (in.)	SAP2000 (Model 1) (in.)	SAP2000 (Model 2) (in.)	Abaqus (in.)	SAP2000 (Model 1) (in.)	SAP2000 (Model 2) (in.)
L1	0.14	0.14	0.14	0.27	0.28	0.28
L2	0.26	0.25	0.26	0.34	0.34	0.34
L3	0.44	0.44	0.45	0.27	0.26	0.26
L4	0.64	0.65	0.65	0.20	0.19	0.19
L5	0.44	0.44	0.45	0.14	0.13	0.13
L6	0.26	0.25	0.25	0.08	0.07	0.07
L7	0.14	0.14	0.14	0.04	0.04	0.04



(a) End View



(b) Side View

Figure 4.1 The Bridge Road over Klamath River

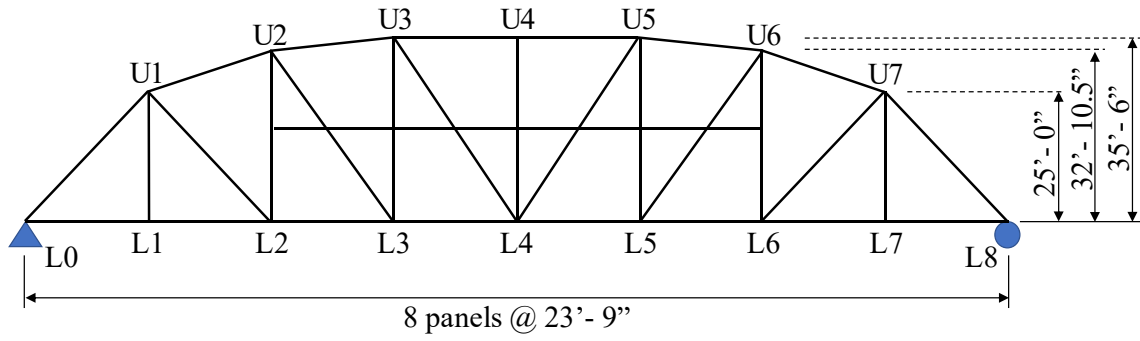


Figure 4.2 Elevation of Truss and Member Designation

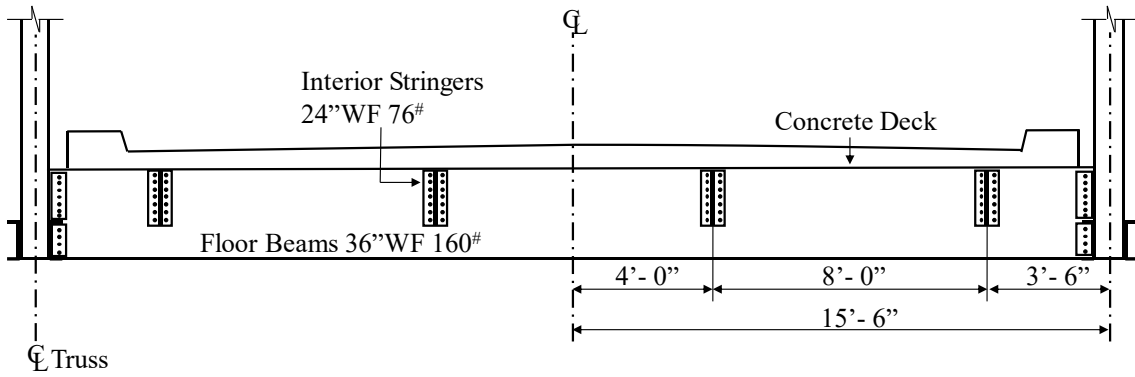


Figure 4.3 Cross Section of Bridge

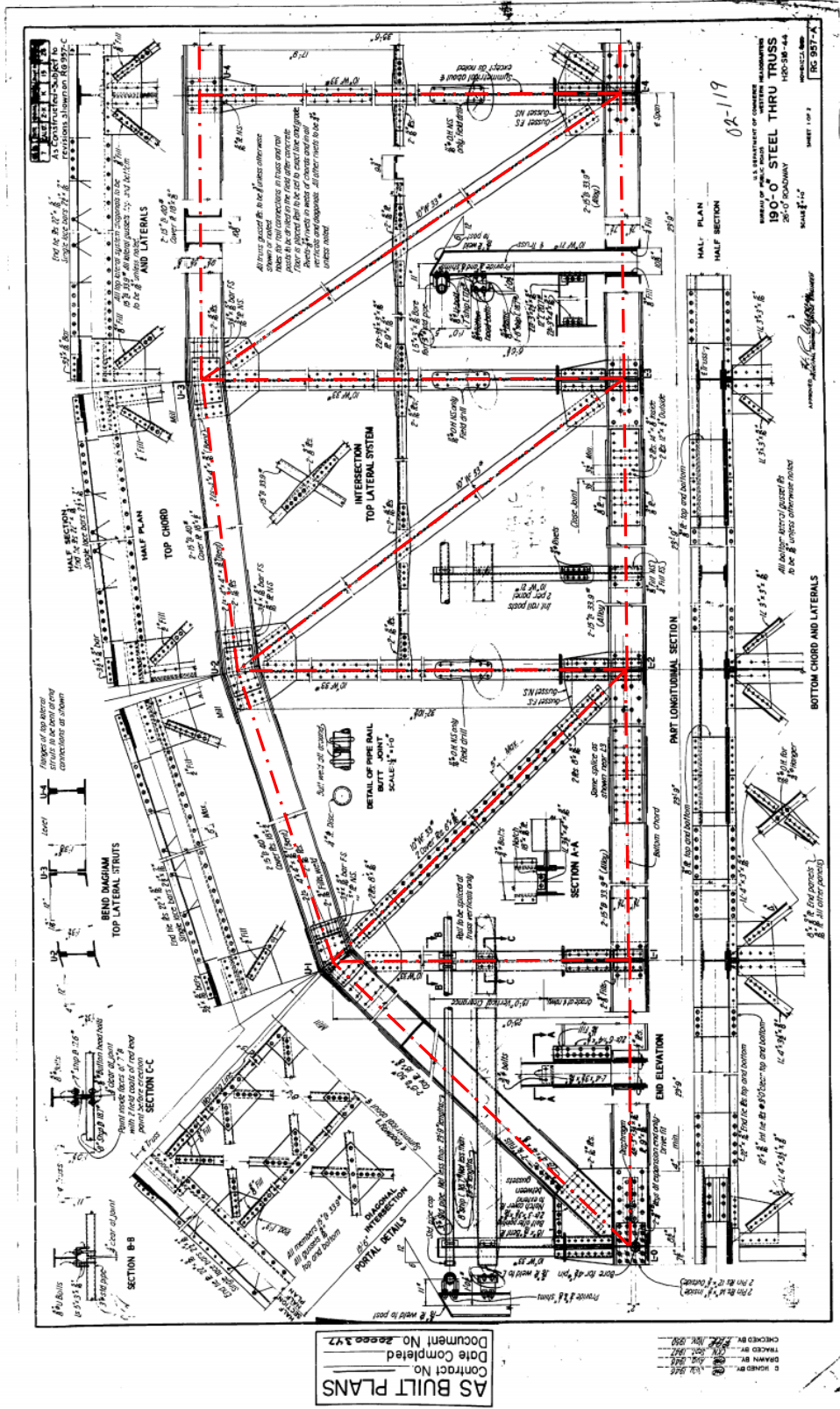


Figure 4.4 As-built Drawing



Figure 4.5 Gusset Joints at U2

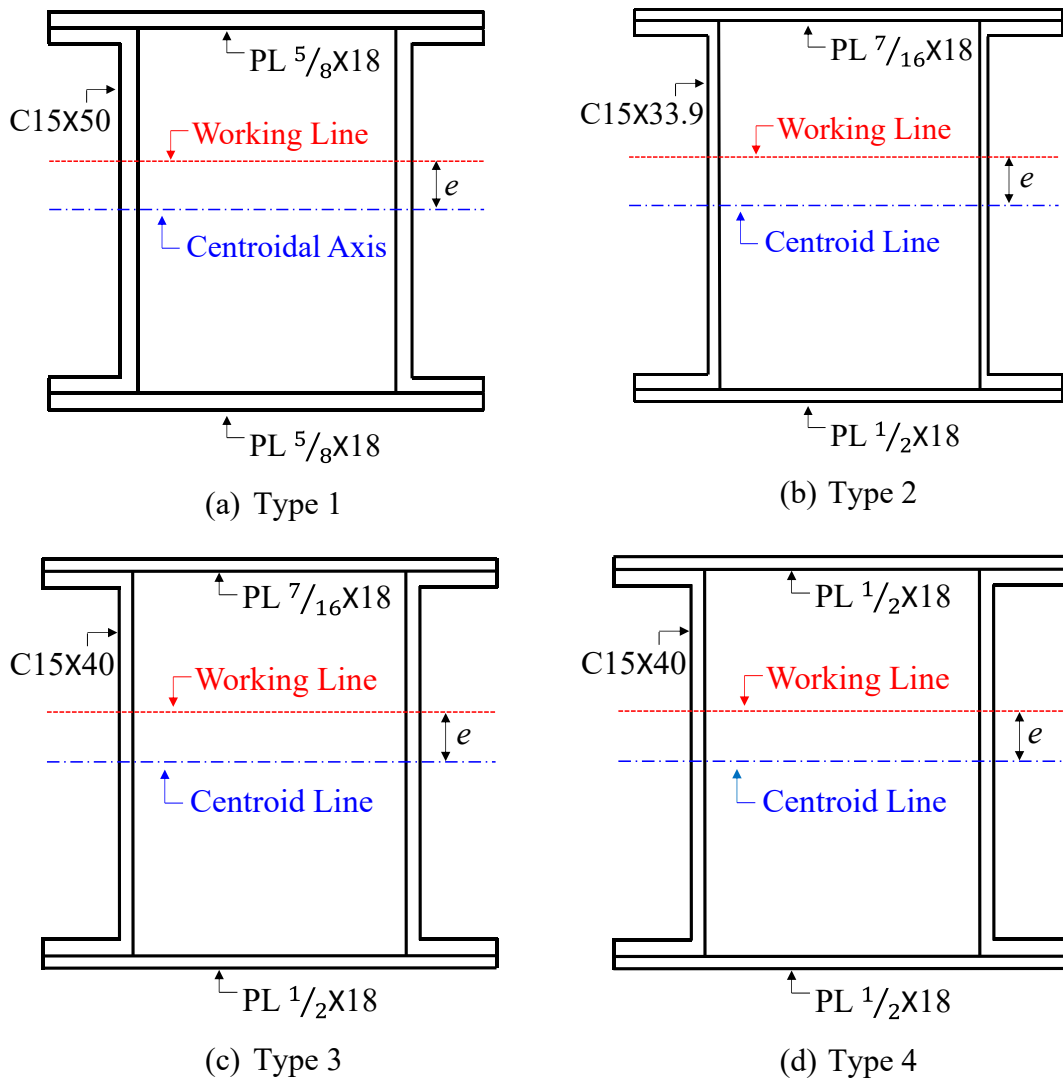
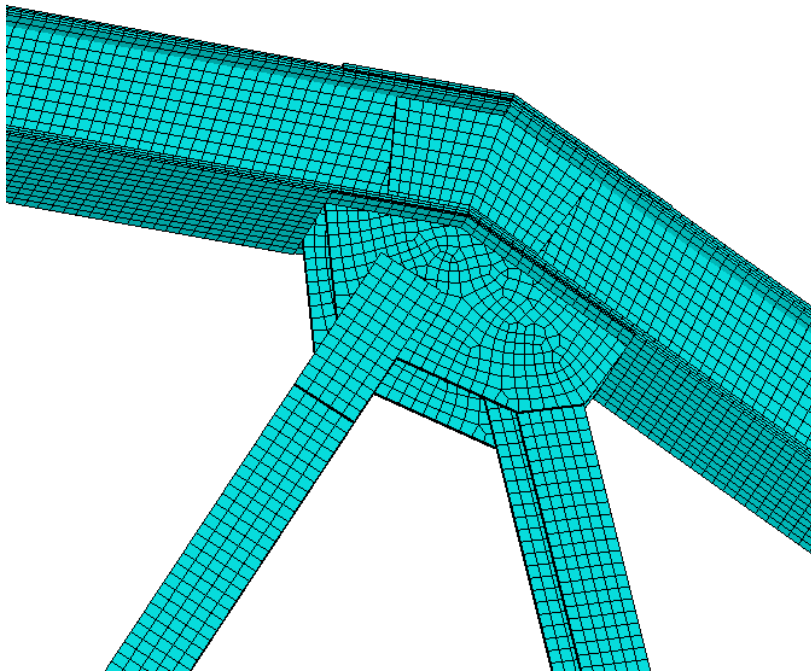


Figure 4.6 Cross Sections of Built-up Members



(a) Actual

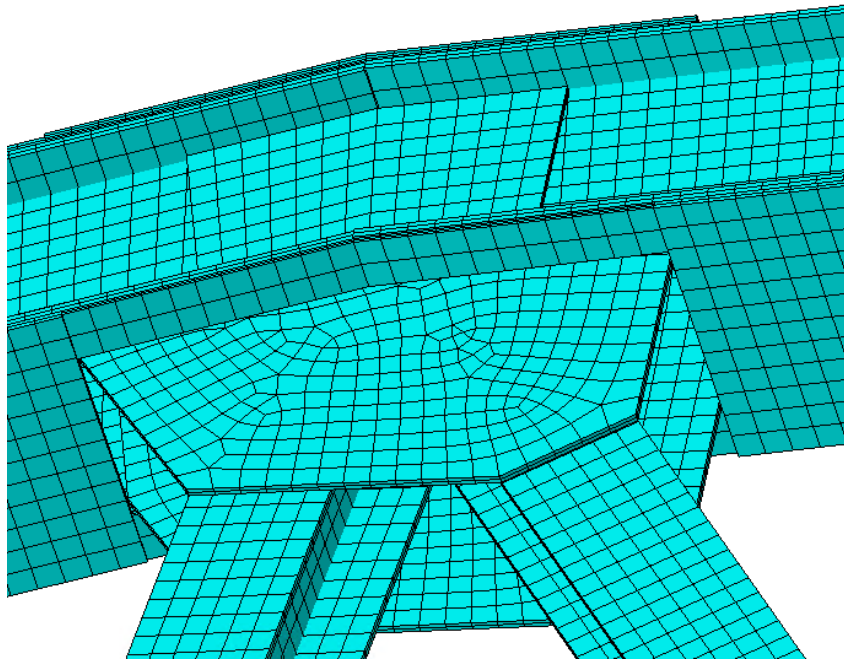


(b) Model

Figure 4.7 Detail at Joint U1

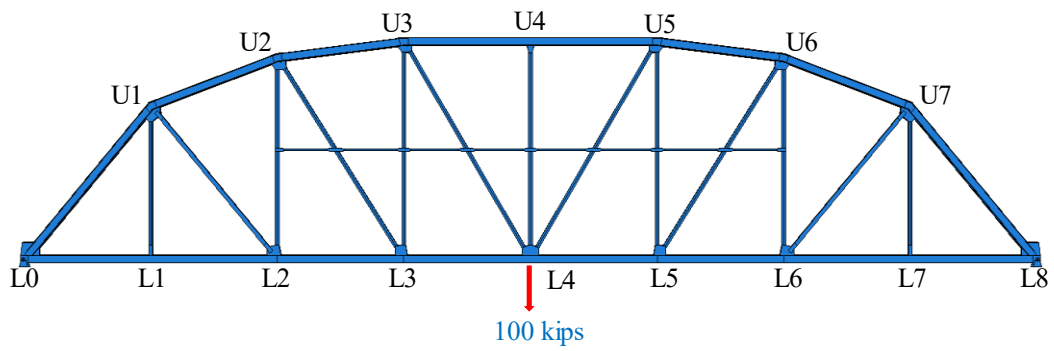


(a) Actual

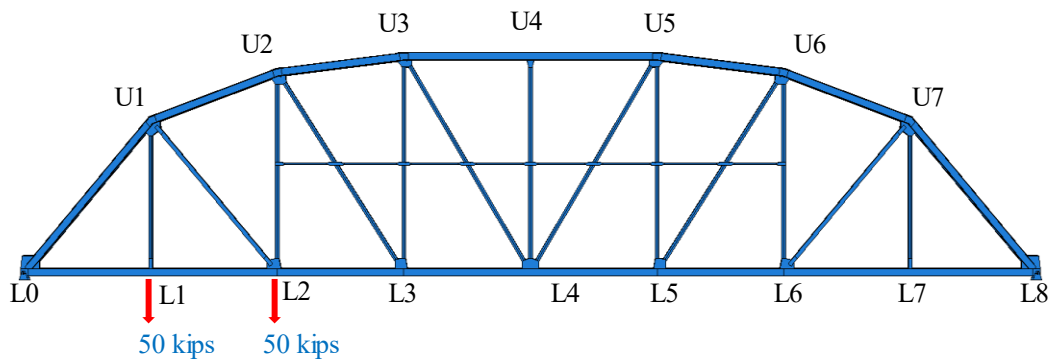


(b) Model

Figure 4.8 Detail at Joint U2

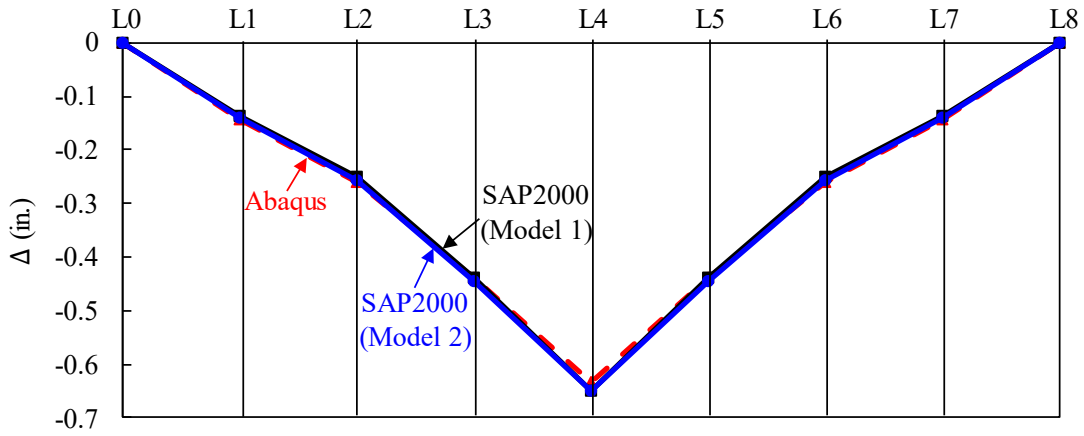


(a) Load Case 1

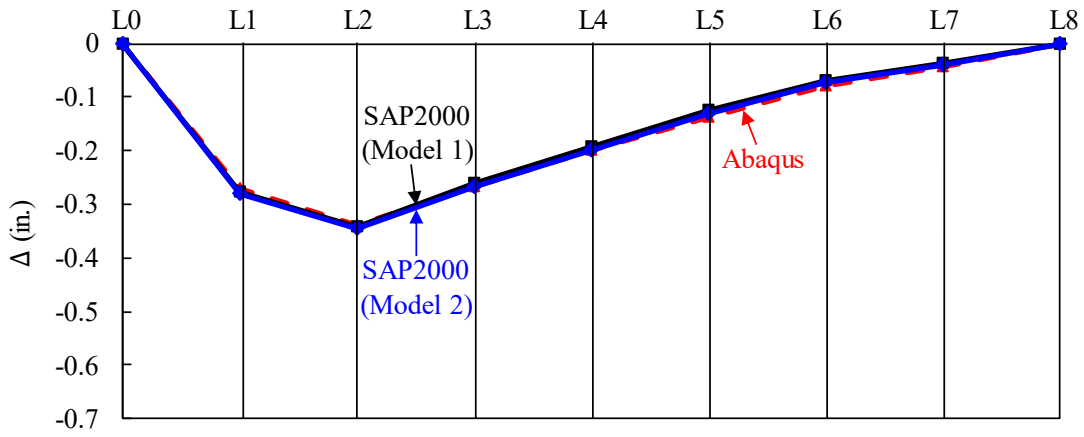


(b) Load Case 2

Figure 4.9 Loading Cases

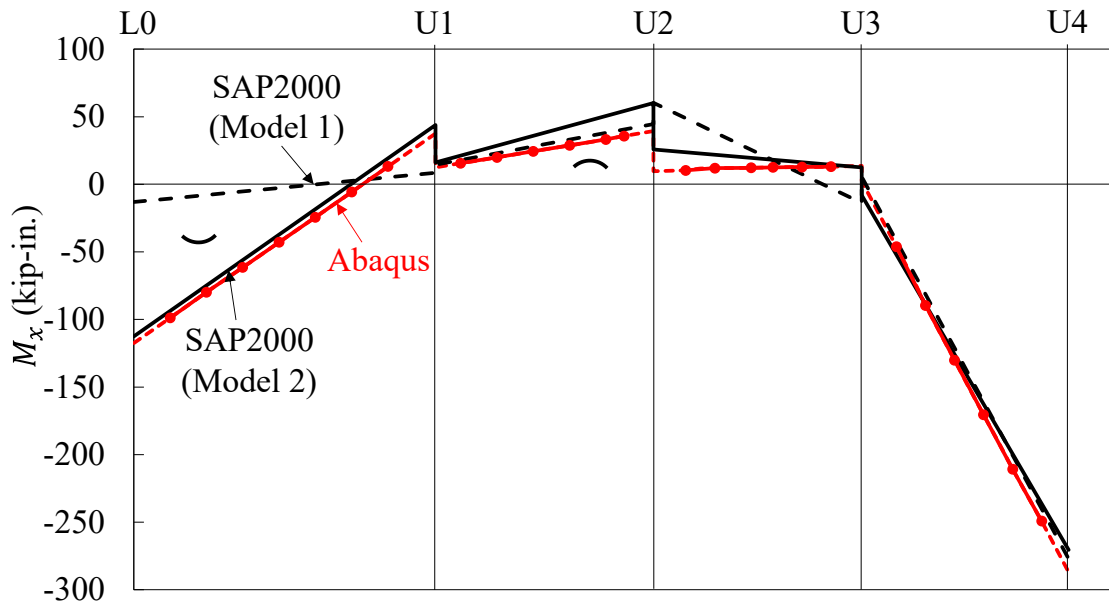


(a) Load Case 1

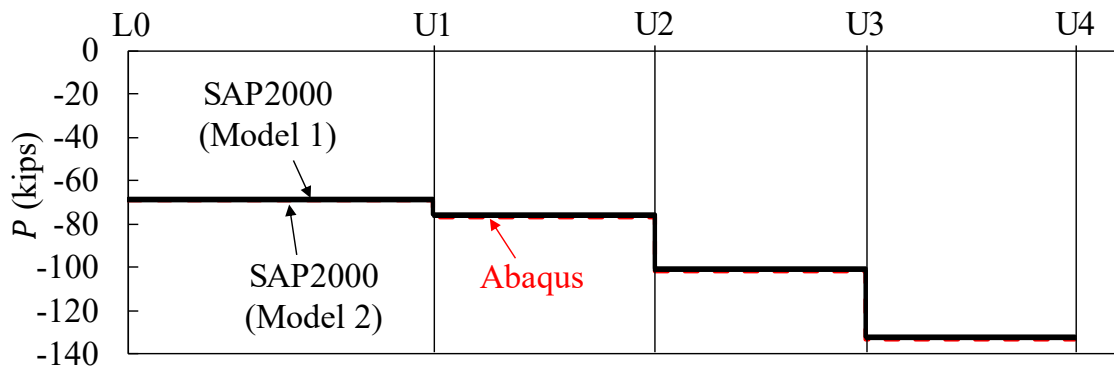


(b) Load Case 2

Figure 4.10 Comparison of Vertical Deflection Profiles

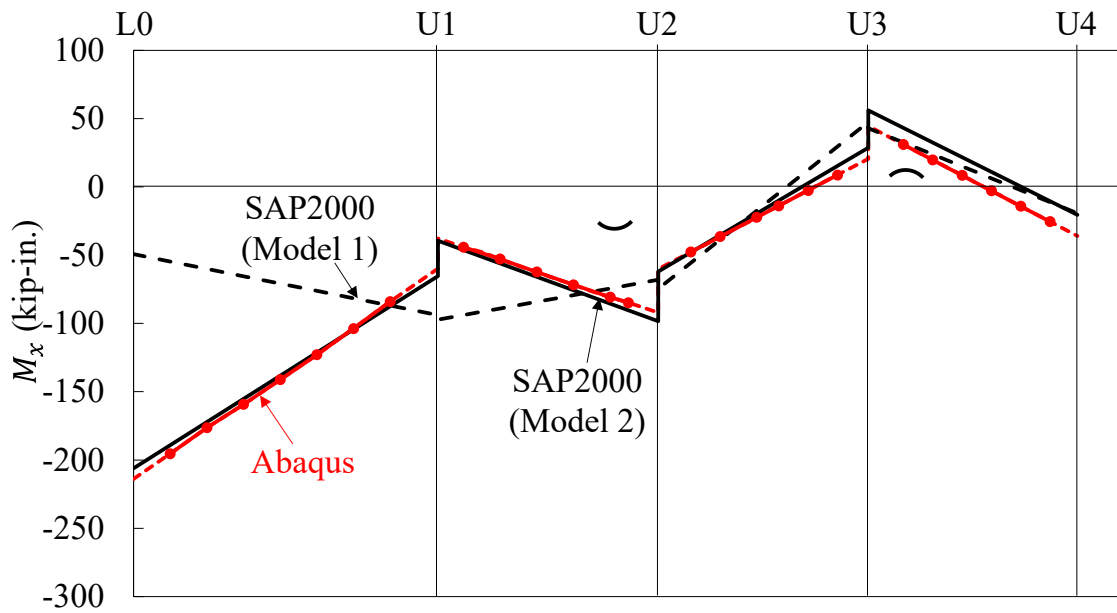


(a) In-plane Moment

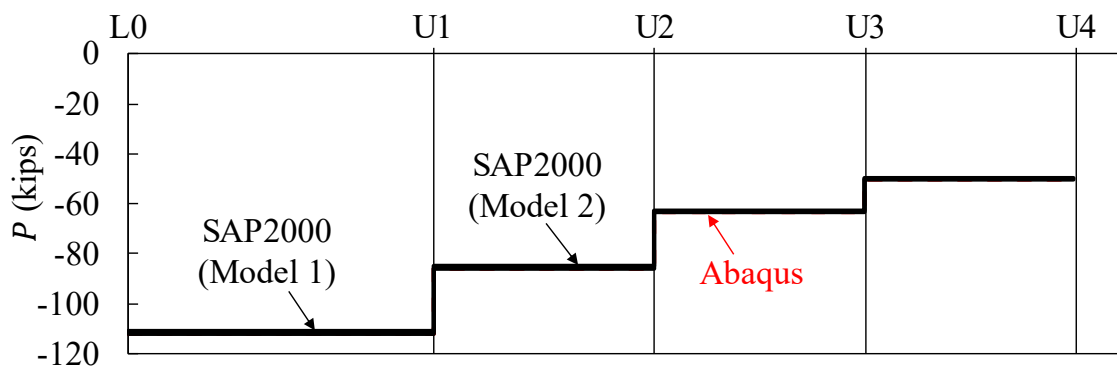


(b) Axial Force

Figure 4.11 Distribution of Moment and Axial Force (Load Case 1)



(a) In-plane Moment



(b) Axial Force

Figure 4.12 Distribution of Moment and Axial Force (Load Case 2)

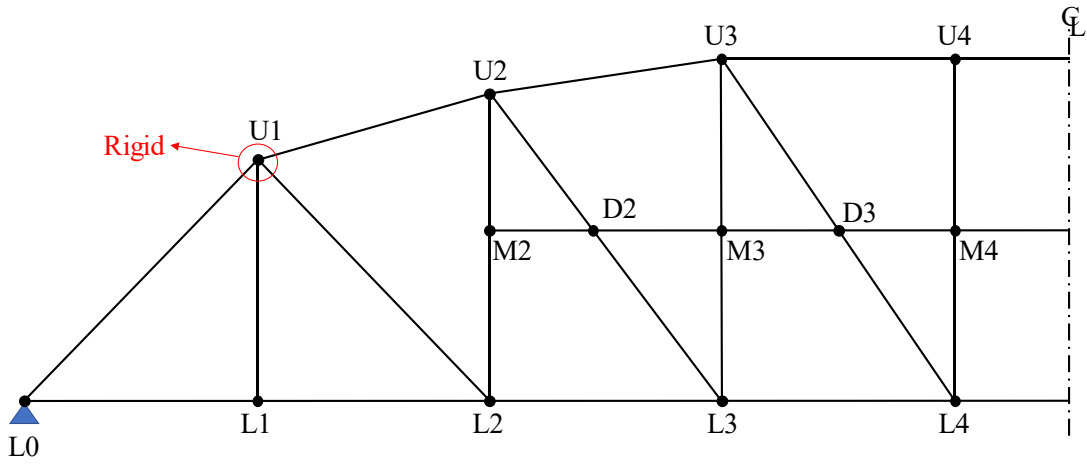


Figure 4.13 SAP2000 Model of the Truss (Model 1)

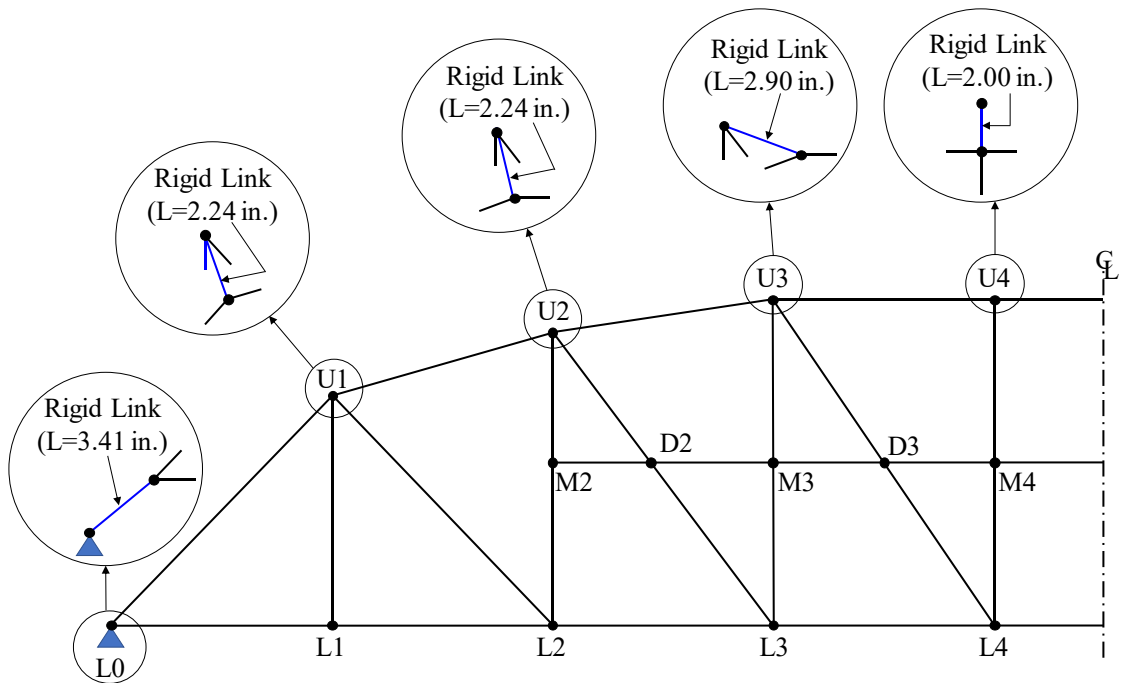


Figure 4.14 SAP2000 Model of the Truss (Model 2)

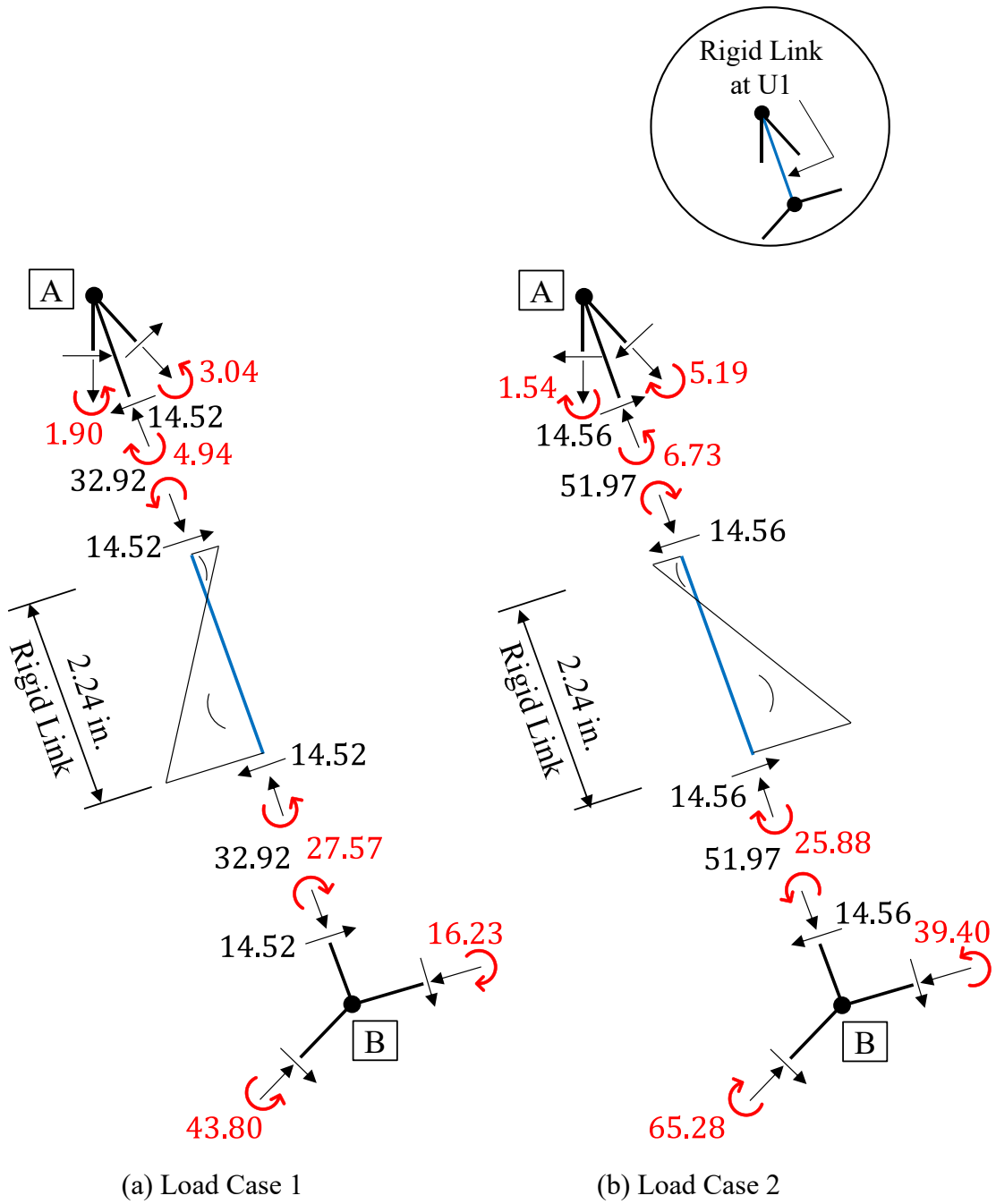
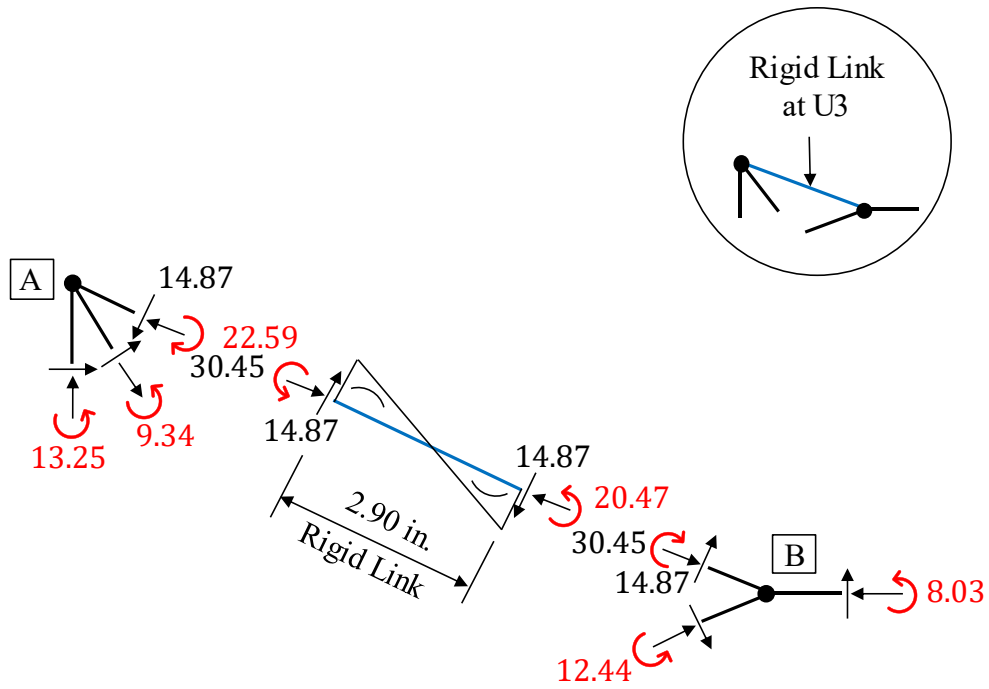
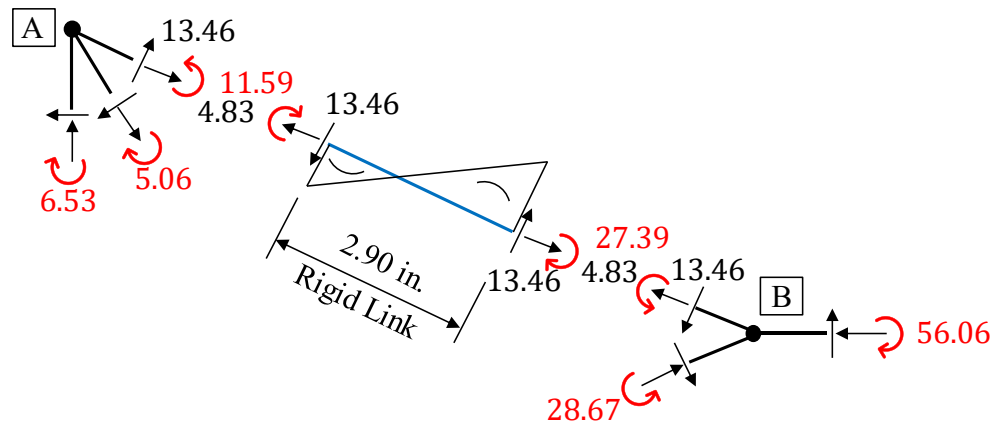


Figure 4.15 Free-body Diagram at Joint U1

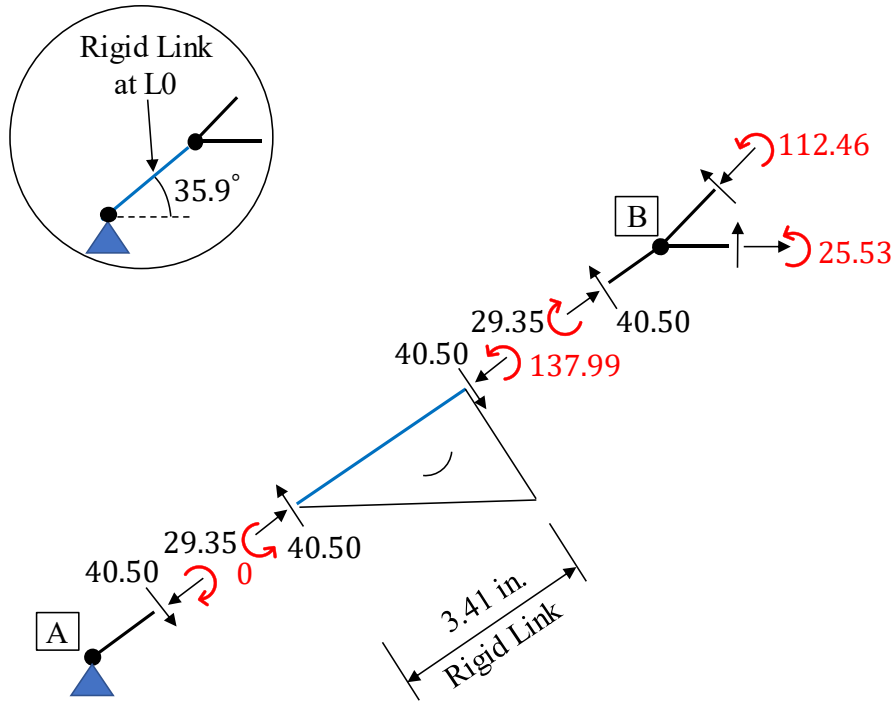


(a) Load Case 1

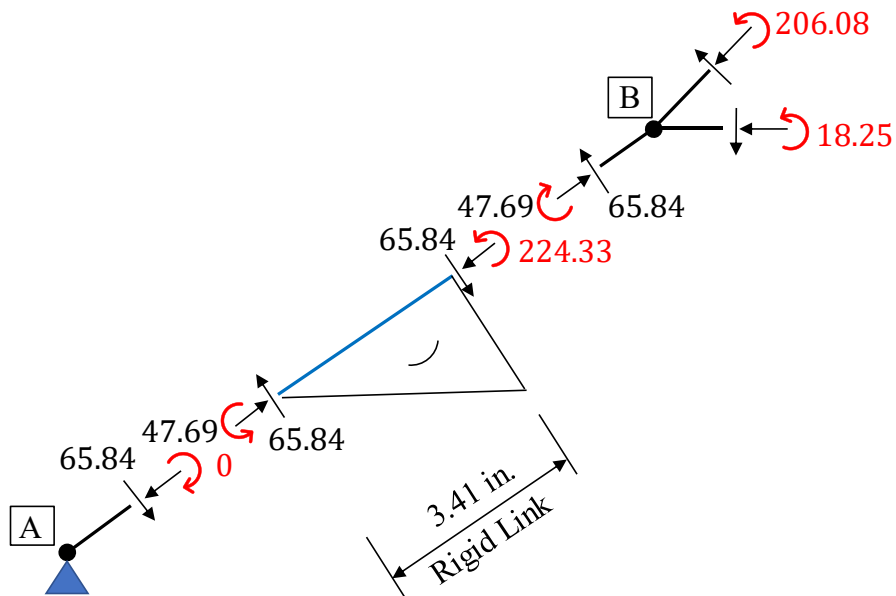


(b) Load Case 2

Figure 4.16 Free-body Diagram at Joint U3

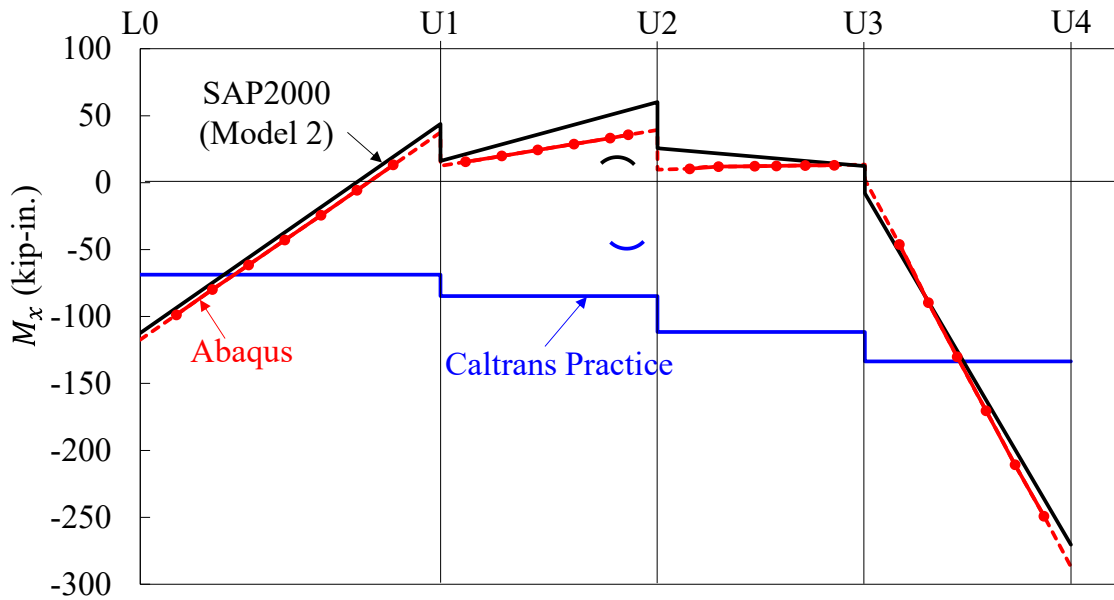


(a) Load Case 1

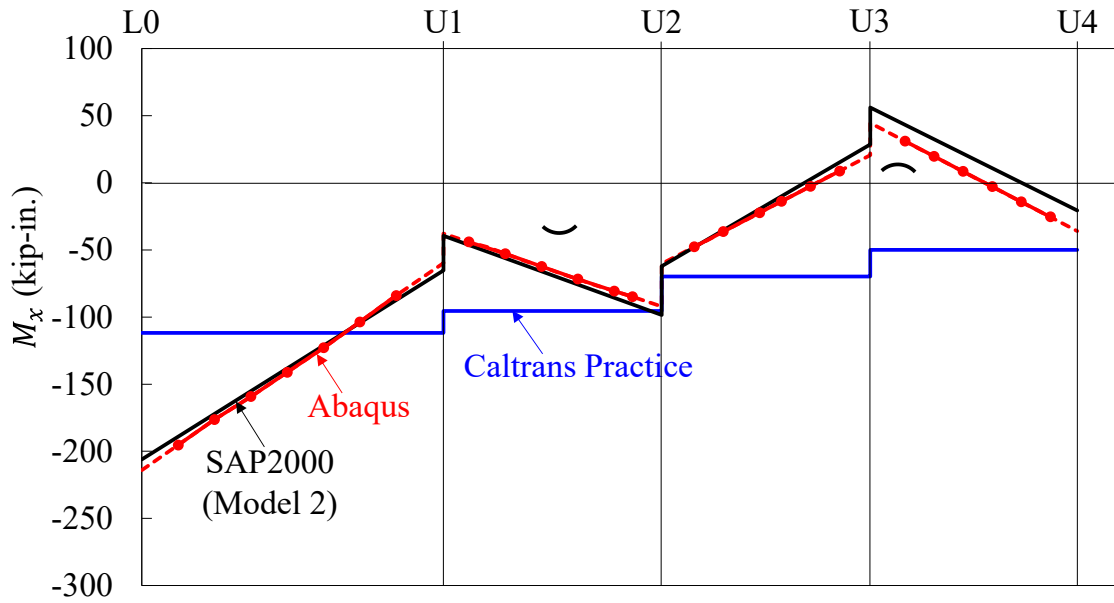


(b) Load Case 2

Figure 4.17 Free-body Diagram at Joint L0

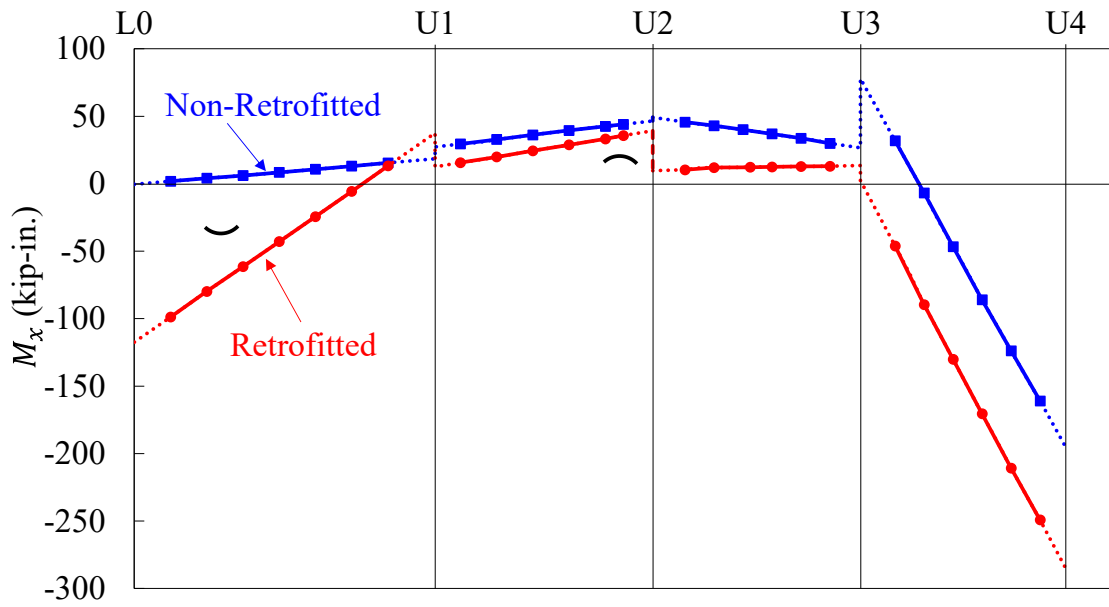


(a) Load Case 1

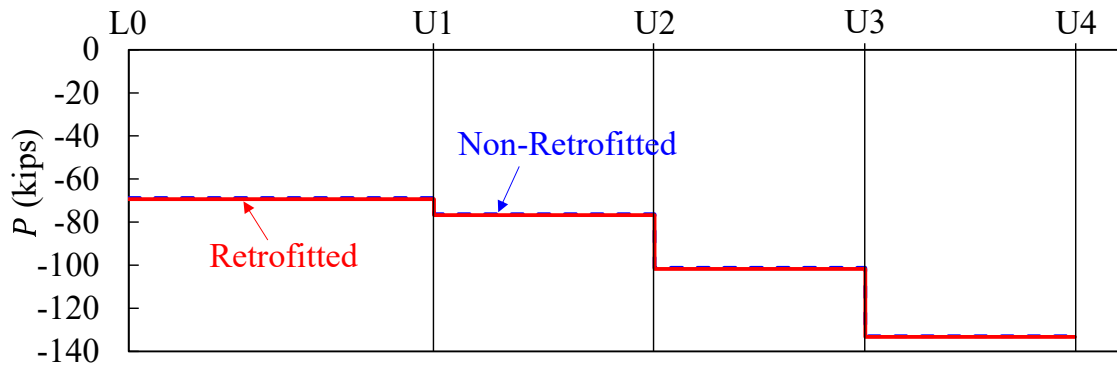


(b) Load Case 2

Figure 4.18 Comparison of Moments Based on SAP2000 and Caltrans Practice



(a) Moment Diagram



(b) Axial Force Diagram

Figure 4.19 Comparison of Retrofitted and Non-Retrofitted

## 5 SUMMARY AND CONCLUSIONS

### 5.1 Summary

Many existing steel truss bridges use built-up members that are connected by either pin connections or riveted gusset connections. The built-up members typically consist of channels and angles spaced apart by continuous or discrete plates. Often the cross sections of built-up members forming the top chord of the truss are not symmetric about the axis of in-plane bending due to the tendency of designers to use solid top cover plates and battens or lacing to brace the bottom of the member. Working lines, when provided in the as-built design drawings, do not necessarily coincide with the centroidal lines, creating an eccentricity,  $e$ , in each truss member. In a structural analysis to evaluate member forces, it is a common practice that a pin-connected truss model be created based on the working lines; such analysis would provide only axial forces in each member. To account for the eccentricity effect in truss members, which produces moments, there is no consensus-based approach.

Two existing single-span steel truss bridges recommended by Caltrans were used to evaluate a common practice used by Caltrans, which uses the full eccentricity for pin-connected members and half the eccentricity for gusset connections, to compute member moments. The pin-connected Bridge Road over Santa Paula Creek, located in Ventura County, was evaluated by both finite element analyses and field testing. Only finite element analyses were conducted on the Bridge Road over Klamath River, located in Siskiyou County, which uses riveted gusset plates to connect members. Two software (Abaqus and SAP2000) were used for the finite element analyses. In the high-fidelity Abaqus finite element model, four-node quadrilateral shell elements were used to model the structure including built-up members with lacing. All rivets and pin connections were also properly simulated. SAP2000, which uses beam elements to model truss members, represents a practical structural analysis software similar to those commonly used in bridge design and evaluation.

## 5.2 Conclusions

### 5.2.1 Pin-connected Bridge Road over Santa Paula Creek

The following conclusions can be made from the study of the pin-connected Bridge Road over Santa Paula Creek.

- (1) When the eccentricity of the members is included in SAP2000, the predicted moment diagram is consistent to that from the Abaqus analysis (Figure 2.21 and Figure 2.22).
- (2) Field testing confirmed the reliability of the software used (Figure 3.13 and Figure 3.14). Specifically, testing confirmed the double-curvature bending of the top chords as predicted by finite element analyses. But member end moments from field tests were lower than those from finite element analyses. Uncertainties in testing (e.g., truck load magnitude and location) and modelling (e.g., frictionless pins assumed in finite element analyses) might have caused such discrepancy.
- (3) Member end moments of the top chord calculated by following the Caltrans practice show no resemblance to those predicted from finite element analyses (Figure 2.23). With the exception of the end post L0U1, this practice cannot reliably predict the moment magnitude, the curvature direction (concave or convex), and single- versus double-curvature. Since this practice would result in uniform bending, the moment magnifier,  $\delta_b$ , will be always larger than 1.0. With the large moment gradient observed in top chord members like U1U2 and U2U3, however, such artificial moment magnification due to the P- $\delta$  effect is unnecessary. Therefore, the Caltrans practice tends to overestimate the P- $\delta$  effect at the member level.
- (4) The Caltrans practice can only provide a reliable prediction of the moment in the end post because (i) the axial force is insensitive to the presence or absence of member-end eccentricity, and (ii) the shear in the rigid link, which is responsible for producing the end moment, is equal to the axial force of the end post (Figure 2.24).

### 5.2.2 Gusset-connected Bridge Road over Klamath River

The following conclusions can be made from the study of the gusset-connected Bridge Road over Klamath River.

- (1) A SAP2000 model (Model 1 in Figure 4.13) that ignores the end eccentricity fails to predict the “actual” moments obtained from the Abaqus analysis (in Figure 4.11 and

Figure 4.12). But a SAP 2000 model (Model 2 in Figure 4.14) that is based on the centroidal lines and considers eccentricity at joints can reliably predict the actual member moments.

- (2) The Caltrans practice again cannot predict the moment gradient observed in the top chord members (Figure 4.18). Taking member U3U4 with Load Case 1 for example, the maximum moment (= 132.3 kip-in.) predicted by the practice is about half the actual value (= 270.5 kip-in.) It also cannot predict the direction of curvature consistently. The uniform moment assumption tends to exaggerate the moment magnification.
- (3) For this bridge, the retrofit scheme with the addition of a bottom cover plate to the top chord members and end post would increase the eccentricity and the associated moments of these members.

### 5.3 Recommended Truss Modeling Procedures

For trusses like the Bridge Road over Santa Paula Creek with (i) members that are pin-connected, and (ii) working lines that pass through steel pins do not coincide with the centroidal axes of the member cross sections, the effect of eccentricity on the first-order moment can be reliably calculated as follows in a computer structural analysis.

- (1) Use the working lines that pass through steel pins to define the geometry of the truss.
- (2) Use beam element to model each member where the eccentricity between the working line and the centroidal axis of the cross section exists. Each beam element is parallel but offset from the working line by a distance  $e$ . Each end of the member is then connected to the pin with a rigid link [e.g., see end post LOU1 in Figure 2.15(b).]
- (3) When a continuous member spans more than two panel joints [e.g., see top chord in Figure 2.15(b)], the beam elements are continuous and are connected to each pin with a rigid link.

For trusses like the Bridge Road over Klamath River with (i) members that are connected with gusset connections, and (ii) the working lines do not coincide with the centroidal axes of the member cross sections, the following procedure is recommended to account for the effect of eccentricity.

- (1) Use the member centroidal axes of the members to define the geometry of the truss.

- (2) If a node created by the intersection of two member centroidal axes does not coincide with the support (e.g., Joint L0 in Figure 4.14), use a rigid link to connect the node to the support.
- (3) For joints like U1 to U3 in Figure 4.14 that have multiple members framing into the same gusset connection, define a node by the intersection of two centroidal axes of the top chord members and another node by the intersection of the vertical and diagonal members. Then connect these two nodes by a rigid link.

The computed first-order moment then can be magnified based on Section 4.5.3.2 in the AASHTO LRFD Specifications to include the  $P-\delta$  effect.

#### **5.4 Future Study**

This research focused on the development of proper procedures to model a bridge truss with members that are either connected by steel pins or gusset connections. The analysis was based on specific loading conditions. In rating of existing bridges, however, vehicle live loads need to be considered. Since it is tedious to calculate the rating factor of a given member multiple times by varying the vehicle location, it is a common practice to use the live load response envelope to compare it with the member capacity in order to compute a rating factor. Note that the information on moment gradient is lost in the response envelope, and this approach tends to underestimate the rating factor. (A higher moment gradient will not only increase the lateral-torsional buckling capacity of the member but also reduce or even eliminate the need to magnify the moment due to the  $P-\delta$  effect.) Compound to this response envelope approach is the use of an assumed eccentricity (e.g., 100% eccentricity for pin-connected members and 50% eccentricity for gusset-connected members) to calculate the assumed uniform moment due to eccentricity.

To evaluate the extent of conservatism or non-conservatism in bridge rating with the Caltrans practice, case study of sample truss bridges is needed. Two analyses are required for each bridge. The first analysis follows the current Caltrans practice that includes the use of live load response envelope and the assumed eccentricity. The second analysis, or the “exact” analysis, uses the recommended truss modelling technique in Section 5.3 to include the effect of actual eccentricity. The response envelope approach is not used; instead, the rating factor is calculated for each specific location of the vehicles. For each member, the largest rating factor is the governing one.

## REFERENCES

- AASHTO. (2017). *Standard Specifications for Highway Bridges*, 18<sup>th</sup> Ed., American Association of State Highway Officials, Washington, D.C.
- Abaqus. (2014). *Abaqus Standard User's Manual*, Version 6.14, Dassault Systemes Simulia Corp.
- CSI. (2019). *SAP2000 v21 Integrated Software for Structural Analysis and Design*, Computers and Structures Inc., Berkeley, California.